

12

NOSC

NOSC TD 400

NOSC TD 400

LEVEL II

AD A 096240

Technical Document 400

APPROXIMATE VLF/LF WAVEGUIDE MODE CONVERSION MODEL

Computer applications: FASTMC and BUMP

DTIC
SECRET
MAR 12 1981
E

JA Ferguson
FP Snyder

18 November 1980

Prepared for
US Coast Guard
Omega Navigation System Operations Detail

Approved for public release; distribution unlimited

NAVAL OCEAN SYSTEMS CENTER
SAN DIEGO, CALIFORNIA 92152

DBG FILE COPY

81 3 11 021



NAVAL OCEAN SYSTEMS CENTER, SAN DIEGO, CA 92152

A N A C T I V I T Y O F T H E N A V A L M A T E R I A L C O M M A N D

SL GUILLE, CAPT, USN

Commander

HL BLOOD

Technical Director

ADMINISTRATIVE INFORMATION

Work was performed under Program Element OGVT, Project USCG (NOSC 532-MP01) by members of the Ionospheric Propagation Branch (Code 5323) and the Tropospheric Assessment Systems Branch (Code 5325) for the US Coast Guard. This document covers work from October 1979 through September 1980 and was approved for publication 18 November 1980.

Released by
JH Richter, Head
EM Propagation Division

Under authority of
JD Hightower, Head
Environmental Sciences
Department

METRIC CONVERSION

<u>To convert from</u>	<u>to</u>	<u>Multiply by</u>
inches	mm	25.4

UNCLASSIFIED

SECURITY CLASSIFICATION OF THIS PAGE (When Data Entered)

20. Abstract (Cont)

BUMP, a program incorporating the FASTMC capabilities, allows for relatively easy modeling of a moving perturbation with a minimum of data preparation. The FASTMC-BUMP combination is designed specifically for consideration of transequatorial vlf propagation.

S N 0102- LF- 014- 6601

UNCLASSIFIED

SECURITY CLASSIFICATION OF THIS PAGE(When Data Entered)

CONTENTS

1. VLF RADIO WAVE PROPAGATION TO GREAT DISTANCES . . . page 3
 Scope of this document . . . 3
 Theoretical developments . . . 3
 The terminator . . . 11
 Equatorial anomaly . . . 13

2. WAVEGUIDE MODE THEORY - HORIZONTALLY HOMOGENEOUS GUIDES . . . 17
 Coordinate transformation . . . 17
 Mode equation . . . 20
 Point sources and line sources . . . 22
 Modal excitation factors and polarization coupling . . . 24

3. WAVEGUIDE MODE THEORY - HORIZONTALLY INHOMOGENEOUS GUIDES . . . 31
 Operator equations . . . 32
 Mode conversion . . . 34

4. FASTMC . . . 48

5. BUMP . . . 60

REFERENCES . . . 67

APPENDIX A: FASTMC . . . 71

APPENDIX B: BUMP . . . 100

Accession For		
NTIS GRA&I	<input checked="" type="checkbox"/>	
DTIC TAB	<input type="checkbox"/>	
Unannounced	<input type="checkbox"/>	
Justification		
By _____		
Distribution/ _____		
Availability Codes		
Dist	Avail and/or Special	
A		

1. VLF RADIO WAVE PROPAGATION TO GREAT DISTANCES

SCOPE OF THIS DOCUMENT

The Omega Navigation System Operations Detail (ONSOD) of the US Coast Guard is responsible for the implementation and evaluation of the Omega Navigation System. Omega uses very low frequency (VLF) radio waves with range from 10.2 to 13.6 kHz and is an operational global system. Thus, a complete evaluation of the system requires an understanding of VLF radio wave propagation under both spatial and temporal operating conditions. A particular set of conditions has been of considerable interest, namely transequatorial propagation at night or during day-night transitions. Theoretical evaluation of such propagation paths requires highly detailed tracking of the propagating modes through the region of the geomagnetic equator because the modes can be very sensitive to the magnetic field. An even more difficult problem is the analysis of the effect of a moving day-night terminator on such paths.

A general background review of VLF radio wave propagation from a theoretical viewpoint is presented, and this is followed by a discussion of transequatorial VLF propagation at night and during day-night transitions. A VLF propagation model which includes consideration of inhomogeneities both in the vertical direction and along the propagation path is then presented. The model includes consideration of the anisotropic effects (caused by the geomagnetic field). It has been implemented into a FORTRAN computer program called FASTMC. This program allows for an arbitrarily oriented and elevated transmitting dipole antenna from which the vertical or horizontal electric field at an arbitrary elevation can be output. An application of the FASTMC capabilities has been further implemented into a program called BUMP, which allows for relatively easy modeling of a moving perturbation with a minimum of data preparation. The FASTMC-BUMP combination is designed specifically for consideration of transequatorial VLF propagation. A discussion of both FASTMC and BUMP is included.

THEORETICAL DEVELOPMENTS

VLF propagation to great distances can be conveniently represented in terms of waveguide mode propagation, where the finitely conducting curved earth and the anisotropic, imperfectly conducting curved ionosphere with dip-

ping magnetic field from the boundaries of a waveguide. The basic idea that the earth and lower ionosphere form a waveguide actually goes back to the work of Watson (1918, 1919), who postulated that the Kennelly-Heaviside layer could be represented as a conducting shell concentric with the spherical conducting earth. Watson developed an exact, slowly convergent, harmonic series-type solution to the EM propagation problem and further devised a transformation of the series to a highly convergent form. The transformation, which involves distortion of the contour of integration in the complex wave number plane, is now identified with Watson's name, although the transformed series is often "rediscovered" by subsequent workers. Although "waveguides" were not really "discovered" until the 1930s, the terms in Watson's transformed series were simply waveguide modes.

The theory of VLF waveguide mode propagation has been presented in the literature in two different formulations. One formulation, based on the pioneering work of Watson (1919) and more recently in the theory given by Schumann (1952, 1954) and developed extensively by Wait (1962), treats the problem in spherical coordinates wherein the fields are expanded in terms of azimuthal, longitudinal, and radial functions. In a sequence of simplifying approximations, including the assumption of azimuthal and longitudinal independence of both ground and ionospheric properties, Wait (1962) develops a modal (eigenvalue) equation in terms of Airy functions. The Airy functions come about as a result of a third-order approximation to spherical wave functions (Watson, 1944). The solution of the eigenvalue equation yields the propagation characteristics of the VLF modes in the earth-ionosphere waveguide, and consideration of orthogonality properties of the radial (Airy) functions yields excitation factors of the modes. The excitation factor is a quantity that gives the amplitude of the wave excited in a given mode by a given source. Another simplifying approximation often made involves the replacement of the inhomogeneous ionosphere with an impedance boundary placed at the height where the bulk of the VLF energy is assumed to be reflected. A similar impedance boundary replacement is also made for the earth. The impedance boundary formulation permits specification of the ratio of an electric field component to a magnetic field component at the boundary without further consideration of the region beyond the boundary. Analytically, formulation in terms of impedance boundaries is equivalent to assumption of "homogeneous boundary conditions" (Friedman, 1959; Morse and Feshbach, 1953). The replace-

ment of an inhomogeneous, isotropic ionosphere by an "equivalent" impedance boundary is a straightforward procedure. Such a replacement for an anisotropic ionosphere is greatly complicated by the coupling of transverse magnetic and transverse electric polarizations. Boundary conditions must then be formulated in terms of an impedance matrix. Unfortunately, the complication is sufficient to render many of Wait's results inapplicable to the highly anisotropic nighttime ionosphere and to limit their application to the daytime ionosphere, for which the effect of anisotropy is slight. The theory has been significantly modified and extended to anisotropic ionospheres by Galejs (1972).

Another formulation of the earth-ionosphere waveguide problem has been presented by Budden (1961a). In this formulation, a modal equation is developed in terms of reflection coefficients of the ionosphere and the earth. Formulation in terms of reflection coefficients permits determination of propagation characteristics of waveguide modes for essentially any ionospheric or ground conditions, limited only by the ability to compute reflection coefficients for the environment considered. Budden's formulation is essentially planar, although he does point out how to include earth curvature in the direction of propagation in an approximate way by modifying the refractive index in the space between the earth and the ionosphere (Budden, 1962). A more rigorous technique was introduced by Richter (1966) and has been employed in VLF propagation studies by Pappert (1968) and Abbas et al (1971). This technique assumes cylindrical stratification and effects a conformal transformation from cylindrical to Cartesian coordinates. Modal excitation values are determined in Budden's formulation by applying of residue theory rather than by using the modal orthogonality properties of conventional waveguide theory employed by Wait.

Whichever formulation is used at the outset, the use of waveguide mode theory leads to specification of the VLF field as a summation of terms called modes. Because most VLF transmitters in common use radiate a vertically polarized field, only the radial or vertical component of the electric field is usually considered. For a time harmonic source, the VLF modesum for the vertical electric field may be written as

$$E_v(d) = \frac{K(P,f)}{\sqrt{(\sin d/a)}} \sum_n \Lambda_n G_n^T G_n^R e^{-ik_0 S_n d}, \quad (1)$$

where $K(P,f)$ is a complex constant dependent on transmitted power (P) and frequency (f), d is the distance from the transmitter on a homogeneous, smooth earth of radius a , Λ_n is the excitation factor for mode n , normalized to unity for flat earth, perfectly conducting boundaries, k_0 is the free space wave number, S_n is the propagation factor, and $G_n^{T,R}$ represents height-gain functions for mode n , normalized to unity at the ground. One height-gain function is needed for the transmitter (T) and one for the receiver (R). Generally, both Λ_n and S_n are complex. The real part of S_n determines the distance dependence of the phase for a mode while the imaginary part of S_n determines the attenuation rate. Thus

$$\begin{aligned} \alpha_n &= -k_0 \text{Im}(S_n) \\ v_n/c &= 1/\text{Re}(S_n), \end{aligned} \quad (2)$$

where α_n is the modal attenuation rate, v_n is the phase velocity, and c is the speed of light in free space.

Numerous assumptions and approximations, some of which will be removed in following sections, are implicit in equation (1). It is assumed that the propagation environment is homogeneous in all but the vertical direction. Thus, the propagation factor, S_n , is independent of position. The influence of the curvature of the earth transverse to the propagation direction is approximately accounted for in the spreading term, $\sin(d/a)$. The energy flux for a wave traveling outwards with cylindrical symmetry on a flat earth without attenuation is proportional to $1/r$. For a spherically curved earth this energy flux would be proportional to $1/\sin(r/a)$. Thus the usual $1/\sqrt{r}$ term for a cylindrical wave is replaced by the $1/\sqrt{\sin(r/a)}$ term. A careful derivation of the mode equation in spherical coordinates, such as that presented by Wait (1962) and discussed previously, yields the $\sin(d/a)$ term as a consequence of an asymptotic approximation to a Legendre function. The mode sum in equation (1) further assumes that "round the world" signals are absent, an approxima-

tion not valid when receiver locations are near the antipode of the transmitter - multipath focusing then occurs.

Extensive results of numerical calculations of VLF waveguide mode constants have been presented in the literature. Early results given by Wait and Spies (1964) show some general properties of VLF modes for typical daytime and nighttime ionospheres, with various ground conductivities and for east-to-west or west-to-east propagation directions at the magnetic equator or when the earth's magnetic field is ignored. In general, the attenuation rate of the lowest order mode is less at night than during the day, and is less for west-to-east propagation than for east-to-west. The attenuation rate increases as ground conductivity decreases - rapidly at low conductivities such as occur for the polar icecaps. Each successive mode order suffers a greater attenuation rate than the previous order mode for both day and night.

Typically, daytime attenuation rates for the first order mode range from 2 to 4 dB/1000 km over the VLF band for sea water ground conditions (essentially equivalent to a perfect conductor at VLF). The nighttime attenuation rates range from about 0.5 to 2 dB/1000 km over the VLF band for the same ground conductivities.

The results of Wait and Spies show that the modal phase velocities for the curved earth can be less than the free space speed of light at intermediate to higher VLF frequencies but increase markedly at lower frequencies. Moreover, phase velocities increase at low ionosphere heights (daytime) compared to higher heights (night), and a decrease in ground conductivity produces a decrease in phase velocity. An increase in phase velocity with mode number is also indicated.

The modal excitation factors and height gains given by Wait and Spies show little dependence on the terrestrial magnetic field. At higher frequencies for isotropic conditions, the excitation factor for the first mode is significantly reduced in comparison with that for a flat earth case. The second mode exhibits a much smaller reduction at higher frequencies. Generally, lower ground conductivities produce an increase in excitation factor. The excitation factor for the second order mode is significantly higher than that for the first order mode, especially at higher frequencies and at night. At night the second order mode may be dominant at the ground to distances of several thousand kilometers. For the first mode the effect of height-gain is

to cause the dominance of the second mode to be greatly diminished or even reversed. This height-gain increase with height for the first order mode has been called the whispering gallery effect by Budden and Martin (1962) or the earth-detached mode by Wait and Spies (1963). It involves successive reflections from the ionosphere with essentially no intermediate bounce at the ground.

The modal constants characterized above become considerably more complicated with full consideration of the geomagnetic field. From the earliest days of VLF, experimental investigation provided evidence of an apparent violation of the reciprocity principle. Round et al (1925), for example, found that VLF radio waves apparently suffered significantly larger attenuation for propagation in a generally easterly direction than in the reverse direction. Some very early results presented by Wait (1961) for sharply bounded model ionospheres suggested that simple harmonic functions may adequately describe the azimuthal dependence of mode constants under daytime conditions. Further, a numerical modeling study by Ferguson (1968) showed that for daytime conditions, only the horizontal component of the geomagnetic field which is transverse to the direction of propagation is important. This component of the magnetic field is the source of nonreciprocity, and the remaining components were commonly assumed only to alter the propagation characteristics somewhat (Makorov et al, 1970). The most severe geomagnetic field effects were thus expected in the equatorial region for propagation across the magnetic meridians.

Perhaps the first indications of extreme complexity in modal behavior due to the geomagnetic field are found in the numerical modeling results of Snyder (1968a, b) and Pappert (1968). Snyder (1968a) addressed the problem of mode numbering for typical nighttime ionospheres as a function of azimuthal variation for a horizontal magnetic field. Results indicated that a mode with lowest west-to-east phase velocity evolved as a result of continuous variation in magnetic azimuth into a mode in the reverse direction with only second lowest phase velocity. Thus, numbering modes in terms of increasing phase velocity, as is commonly done, results in the evolution of the first order west-to-east mode into the second order mode in the opposite direction, and vice versa. Further analysis (Snyder, 1968b) indicated that for a certain inclination of a dipping geomagnetic field and at a specific (near north-south) azimuth, the two modes considered above became degenerate, forming a single mode. For inclinations more nearly horizontal than the degenerate

conditions, mode numbering inconsistencies resulted; but for more nearly vertical inclinations, inconsistencies in mode numbering vanished. Pappert (1968) presented the results of numerical modeling for easterly propagation at midlatitudes. Assuming a vertical dipole exciter, Pappert found that, at the high frequency end of the VLF band (only near 30 kHz), modes which are principally transverse electric (TE) may be of importance in a mode sum. Note that a TE mode can be excited by a vertical dipole only because of the presence of the geomagnetic field.

Snyder and Pappert (1969) extended the analysis to consider both easterly and westerly midlatitude nighttime propagation throughout the VLF band as well as to include azimuthal dependencies of mode parameters for a central VLF frequency at both middle and equatorial latitudes. It was found that the importance of principally TE modes is much more pronounced for westerly propagation at midlatitudes than for easterly and that the influence of the principally TE modes on the mode sum can be significant at frequencies as low as 20 kHz or less for westerly propagation. Azimuthal anomalies included drastic polarization changes in going from easterly to westerly paths. For transverse propagation at the magnetic equator, it was shown that modes which are pure transverse magnetic (TM) for propagation to the east may be pure TE for propagation to the west. This is tantamount to the statement that modes which have dominant excitation for easterly propagation may have vanishingly small excitation for westerly propagation. Azimuthal dependencies are characterized by rapid variation of the mode constants in the neighborhood of north-south or south-north propagation, for both equatorial and middle latitudes. These variations manifest themselves in marked differences in mode sums for azimuthal changes as small as 10° or less. Further, it was shown that the maximum total signal attenuation occurs for north-south propagation rather than for east-west propagation.

Although Snyder and Pappert (1969) used hypothetical ionospheres, their results have been further substantiated by Foley et al (1973), who used "realistic models of the ionosphere." Foley et al essentially duplicated the analysis of Snyder and Pappert but used ionospheric models presented in the literature by Deeks (1966) and Smith et al (1968). Foley et al concluded that mode characteristics are dependent on the ionosphere model assumed. For example, results with the Smith profile were similar to the results of Snyder and Pappert, whereas under certain circumstances results differed with the Deeks profile. For propagation in the north-south direction with the Deeks

profile, anomalies were found in the behavior of modes 1 and 2. It would appear that between 16 and 20 kHz, modes 1 and 2 interchange their identities. Although unknown to Foley et al, this identity interchange would seem to be just another manifestation of the modal degeneration reported by Snyder (1968b).

THE TERMINATOR

A manifestation of multimode propagation is found in the phenomenon of sunrise and sunset fading, which is characterized by periodic and repeatable variations in amplitude and phase as the dawn-dusk terminator moves along a VLF propagation path. Crombie (1964) explained the phenomenon using waveguide mode concepts. Of all possible combinations of conditions — sunrise and sunset, position of terminator on propagation path, relative positions of transmitter and receiver, etc — only two fundamental situations occur within the confines of Crombie's explanation.

The first situation depicts the field incident on the terminator from the transmitter as determined by two modes, and the field at the receiver as determined by only one mode. This situation would be characteristic of a transmitter on the night side of the terminator and the receiver on the day side sufficiently removed to avoid multimode propagation. The received signal then depends on the amplitude and phase relationships of the modes incident on the terminator and on the efficiency with which these modes are converted by the terminator to the single mode which reaches the receiver. Because the modal relationships are determined by the distance of the terminator from the transmitter, periodic variations will occur in the received signal as the terminator moves along the propagation path. The periods will be determined by the difference in the phase velocities of the two modes entering the terminator, and the variations must occur simultaneously for all points in the portion of the propagation path beyond the terminator region. The fading would be most intense when the two entering modes have the most pronounced interference — usually when the terminator is near the transmitter.

The second situation depicts the incident field as a single mode. The presence of the terminator leads to multimode generation in the region past the terminator, which in turn leads to modal interference. In this situation, the interference pattern would appear to be attached to the terminator and to move synchronously with it. Signal minima are then to be expected at fixed distances from the terminator, the distance between fades being determined by the difference between the phase velocities of the two modes leaving the terminator region. The deepest signal fades would be expected as the terminator approaches the receiver. This situation corresponds to propagation from the sunlit side of the terminator into the night side. Note that in both

situations, the fade spacing would be determined by the differences between the phase velocities of two nighttime modes.

A thorough experimental examination of the Crombie model was conducted by Walker (1965), who recorded 18 kHz transmissions from NBA Balboa, Panama, while making repeated shipboard crossings of the Atlantic in the equatorial region. During sunrise (propagation from night to day) signal fades were observed simultaneously at all points in the day portion of the path — in agreement with the first situation discussed above. Walker determined the change in terminator position between successive fades and from this calculated the required differences in the phase velocities of the two interfering modes. These results were in good agreement with theoretical results for nighttime ionospheres, further substantiating the Crombie model. Observations were also made during sunset (propagation from day to night) and results were in excellent agreement with the Crombie model.

EQUATORIAL ANOMALY

The observations just discussed were, for the most part, made at middle or low latitudes. As the previous discussion indicates, such observations have been explained adequately by the use of quite simple VLF waveguide mode theory. However, some observations of VLF transmissions over long transequatorial paths have apparently indicated an anomalous effect associated with nighttime or transitional transequatorial VLF propagation.

Of the reports on transequatorial VLF propagation, one of the earliest to show an apparent anomaly was by Chilton et al (1964). They made simultaneous observations of NBA transmissions (Canal Zone, Panama) at 18 kHz for paths to both the northern and southern hemispheres. Both paths were of similar length, but the southern hemisphere path crossed the magnetic equator. Although they did not look at transition fading, they did observe an anomalous difference in the diurnal changes of signal amplitude and phase. Chilton et al suggested that their observations resulted from a difference in ionization profile due to latitudinal dependence of cosmic rays. More recently, Chilton and Cray (1971) suggested that the latitude-dependent ionization source might arise from the recently discovered x-ray stars.

Araki et al (1969) recorded dual frequency (15.5 and 22.3 kHz) VLF signals in Japan from station NWC in Australia. They reported sunrise fading on 22.3 kHz but not on 15.5 kHz and further noticed that during fading at 22.3 kHz the first phase change was an increase followed by a phase decrease. The nighttime field strength was somewhat less at 15.5 kHz and somewhat higher at 22.3 kHz than during the day. Araki et al (1969) concluded that their results suggest the existence of a frequency-dependent anomaly of the nighttime field relative to the daytime field along their transequatorial propagation path.

Bickel et al (1970) conducted an experiment to investigate the apparently anomalous results of Snyder and Pappert (1969), who predicted maximum signal attenuation in a southerly rather than westerly direction. Measurements of 23.4 kHz signals from station NPM (Lualualei, Hawaii) were made aboard an airplane as it flew radials along the propagation paths to Seattle, Ontario (California), Samoa, and Wake Island. Bickel et al confirmed the Snyder and Pappert (1969) results and concluded that the increased southerly attenuation is an effect of the geomagnetic field. An unexplained effect, however, was observed. For the radial to Samoa, rapid signal amplitude variations with

distance were observed in the vicinity of the geomagnetic equator. Although equipment problems may be suspected, other Hawaii-based transmissions simultaneously recorded by means of completely separate equipments displayed similar results (Bickel, private communication, 1970).

The first report of an equatorial anomaly associated with transition fading was made by Lynn (1967). He reported on VLF transmissions at 18.6 kHz from NLK (Jim Creek, Washington) to Smithfield, South Australia. This propagation path is approximately 13 500 km long, and the receiver-to-geomagnetic-equator distance along the path is approximately 5700 km. The direction of propagation is essentially southwesterly. The interference distance reported by Lynn for sunrise transition fading is approximately 2000 km for the terminator located in midlatitudes (in excess of $\pm 20^\circ$ from the geomagnetic equator). Whenever sunrise transition fading was observed while the terminator was within $\pm 20^\circ$ of the geomagnetic equator, the interference distance increased to as much as 3700 km; and when averaged over the anomaly, it had a value of 2900 km. Lynn (1967) concluded from his observations that the change in interference distance resulted from a change in the difference of phase velocity for two modes as well as from a change in the relative phases of the appropriate mode conversion coefficients. He left unanswered the question of a possible cause for these changes. It is interesting to note that Lynn's conclusions are dependent on his selection of both a VLF propagation model and a mode conversion model. Lynn (1967) assumed an isotropic propagation model wherein any changes in propagation parameters necessitates changes in ionospheric conditions.

Kaiser (1968) examined VLF signals at 18.6 and 24 kHz from NLK and at 20 kHz from WWVL, received at Lower Hutt, New Zealand. These propagation paths are similar to the path considered by Lynn (1967), and Kaiser's results are much the same as Lynn's. An anomalously large interference distance (in excess of 3000 km) was observed for sunrise transition fading when the terminator was within about $\pm 20^\circ$ of the magnetic equator. Kaiser also examined transition fading data previously published elsewhere and concluded that anomalously large values of the sunrise interference distance are characteristic of generally east-to-west VLF propagation below about 30° magnetic latitude. A further conclusion by Kaiser (1968) is that any anomaly in sunset transition fading for such paths is relatively minor. Kaiser suggests that a

possible cause of the anomaly might be a larger and sharper day-night waveguide transition near the geomagnetic equator as compared to higher latitudes. He does not suggest, however, a possible cause for the latitudinal dependence of the day-night waveguide transition.

Additional observations of this transition fading anomaly have been reported by Lynn (1969, 1970). These observations further substantiate the general characteristics of the anomaly. A theoretical interpretation of the transequatorial anomaly was presented by Lynn (1970). His interpretation is based only on assumed latitudinal variations in modal phase velocities and relative phases of the mode conversion coefficients. He does not suggest a possible cause for the variations.

Meara (1973) has extended Lynn's (1970) analysis to include determination of the changes in phase velocities within the equatorial anomaly region. He concludes that the phase velocity of the first mode is essentially unaltered by propagation through the equatorial region, whereas that of the second mode is reduced. Note that Meara's results are entirely dependent on the assumed propagation and mode conversion models. Once again, no explanation of a possible cause for the variations in phase velocities is given.

A further application of Lynn's (1970) analysis to explain some anomalous diurnal changes in transequatorial VLF propagation has been made by Araki (1973). The analysis follows essentially that previously discussed. Araki does go a step further than Lynn (1970) and Meara (1973), however, in that he assumes the validity of the isotropic propagation model and asserts that any change in propagation parameters results from a modification of the nighttime equatorial ionosphere. Lynn (1978) has pointed out that the propagation paths of Chilton et al (1964) and Araki (1973) have a west-east component rather than an east-west component as have the other paths discussed here. He further claims that only a minor azimuthal variation in relative phase velocities of interfering nighttime modes can account for the observations of Chilton et al (1964) and Araki (1973). Lynn (1978) thus concludes that the observations of Chilton and Crary (1971) cannot be seen as direct evidence for the control of night VLF reflection heights by stellar X-ray sources. But Svennesson and Westerlund (1979), using waveguide mode theory combined with nighttime profiles given by ionospheric theory, claim results that support the reports of X-ray star effects on VLF radio signals.

To address the question of transequatorial VLF propagation at night or during transition periods requires theoretical VLF radio wave propagation modeling that includes consideration of inhomogeneities along the propagation path as well as in the vertical direction. Anisotropic effects due to the geomagnetic field must also be considered. A propagation model with these capabilities has been developed and is discussed in the following sections.

2. WAVEGUIDE MODE THEORY — HORIZONTALLY HOMOGENEOUS GUIDES

COORDINATE TRANSFORMATION

A review of the waveguide mode theory for VLF propagation in the earth-ionosphere waveguide, homogeneous in and transverse to the direction of propagation, is presented in this section. The earth-ionosphere guide is modeled as cylindrical, with effects of curvature transverse to the direction of propagation accounted for through the use of an appropriate "spreading term" as described in Section 1. Also, as mentioned there, the formulation employed in this study is based on the pioneering work of Budden (1961, 1962). Because Budden's formulation is essentially planar, a coordinate transformation is employed to convert between cylindrical geometry and planar geometry. The transformation, introduced by Richter (1966) with respect to earth flattening techniques and used by Pappert (1968) and Abbas et al (1971) in VLF propagation studies, is briefly outlined.

Application of the conformal coordinate transformation of the form $\rho = ae^{z/a}$; $\phi = x/a$ results in the conversion of circles ($\rho = \text{constant}$) in the ρ, ϕ plane to straight lines ($z = \text{constant}$) in the x, z plane. If a represents the radius of the earth, the transformation maps the surface of the earth ($\rho = a$) to the line $z = 0$. The transformation further maps radii ($\phi = \text{constant}$) from the ρ, ϕ plane to lines $x = \text{constant}$ in the x, z plane. A full circular arc ($\phi = 2\pi$) at $\rho = 0$ is mapped so that the length of x is the circumference of the earth.

The transformation used here differs from that employed by Richter (1966), Pappert (1968), and Abbas et al (1971) in that they maintained some selected altitude (h) as invariant in both coordinate frames. However, the two transformations differ only in quantities of second order in smallness. As the invariant altitude (h) approaches zero, the two transformations become identical.

Maxwell's curl equations with time variation of the form $e^{i\omega t}$ for a medium characterized by a dielectric tensor may be written as

$$\begin{aligned}\nabla \times \underline{E} &= -ik_0 \underline{H} \\ \nabla \times \underline{H} &= ik_0 \underline{\epsilon} \cdot \underline{E},\end{aligned}\tag{3}$$

where k_0 is the wave number of free space ($k_0 = \omega/c$) and $\underline{\epsilon}$ is the dielectric tensor. In equations (3), the variable \underline{H} is actually the magnetic intensity multiplied by the free space impedance. Assuming $\partial/\partial y = 0$, equation (3) in cylindrical coordinates may be written

$$\frac{1}{\rho} \frac{\partial \underline{Y}}{\partial \phi} = -ik_0 H_\rho; \quad \frac{1}{\rho} \frac{\partial \underline{Y}}{\partial \phi} = ik_0 (\underline{\epsilon} \cdot \underline{E})_\rho$$

$$\frac{\partial \underline{Y}}{\partial \rho} = ik_0 H_\phi; \quad \frac{\partial \underline{Y}}{\partial \rho} = -ik_0 (\underline{\epsilon} \cdot \underline{E})_\phi \quad (4)$$

$$\frac{1}{\rho} \frac{\partial}{\partial \rho} (\rho \underline{E}_\phi) - \frac{1}{\rho} \frac{\partial \underline{E}_\rho}{\partial \phi} = -ik_0 H_y; \quad \frac{1}{\rho} \frac{\partial}{\partial \rho} (\rho H_\phi) - \frac{1}{\rho} \frac{\partial H_\rho}{\partial \phi} = ik_0 (\underline{\epsilon} \cdot \underline{E})_y$$

Applying the coordinate transformation to equation (4):

$$\frac{\partial \underline{Y}}{\partial x} = -ik_0 \frac{\rho}{oa} H_\rho; \quad \frac{\partial \underline{Y}}{\partial x} = ik_0 \frac{\rho}{oa} (\underline{\epsilon} \cdot \underline{E})_\rho \quad (5a)$$

$$\frac{\partial \underline{Y}}{\partial z} = ik_0 \frac{\rho}{oa} H_\phi; \quad \frac{\partial \underline{Y}}{\partial z} = -ik_0 \frac{\rho}{oa} (\underline{\epsilon} \cdot \underline{E})_\phi \quad (5b)$$

$$\frac{\partial}{\partial z} \frac{\rho}{a} H_{\phi} - \frac{\partial}{\partial x} \frac{\rho}{a} H_{\rho} = ik_0 \frac{\rho^2}{a^2} (\underline{\underline{\epsilon}} \cdot \underline{\underline{E}})_y; \quad (5c)$$

$$\frac{\partial}{\partial z} \frac{\rho}{a} E_{\phi} - \frac{\partial}{\partial x} \frac{\rho}{a} E_{\rho} = -ik_0 \frac{\rho^2}{a^2} H_y.$$

By making the identifications

$$\begin{aligned} E_x &= \rho/a E_{\phi}; & E_y &= E_y; & E_z &= \rho/a E_{\rho}; \\ H_x &= \rho/a H_{\phi}; & H_y &= H_y; & H_z &= \rho/a H_{\rho}, \end{aligned} \quad (6)$$

equations (5) become identical to what would be obtained in a rectangular coordinate frame for a medium characterized by permeability tensor and dielectric tensor of the form

$$\underline{\underline{\mu}} = \begin{pmatrix} 1 & 0 & 0 \\ 0 & e^{2z/a} & 0 \\ 0 & 0 & 1 \end{pmatrix} \quad (7)$$

$$\underline{\underline{\epsilon}} = \begin{pmatrix} \epsilon_{\phi\phi} & e^{z/a} \epsilon_{y\phi} & \epsilon_{\rho\phi} \\ e^{z/a} \epsilon_{\phi y} & e^{2z/a} \epsilon_{yy} & e^{z/a} \epsilon_{\rho y} \\ \epsilon_{\phi\rho} & e^{z/a} \epsilon_{y\rho} & \epsilon_{\rho\rho} \end{pmatrix}. \quad (8)$$

Some additional insight is obtained by considering the transformed equations in the free space region between the earth and the ionosphere. Making the usual substitutions into equation (5c) from equations (5a) and

(5b), along with the free space assumption, yields the equations

$$\left(\frac{\partial^2}{\partial z^2} + \frac{\partial^2}{\partial x^2} \right) E_y = -k_o^2 e^{2z/a} E_y \quad (9a)$$

$$\left(\frac{\partial^2}{\partial z^2} + \frac{\partial^2}{\partial x^2} \right) H_y = -k_o^2 e^{2z/a} H_y \quad (9b)$$

Thus, the effect of the transformation is to replace the original cylindrical free space region with a planar region filled with a medium which has refractive index equal to $e^{z/a}$ for TE polarized waves or which has permeability equal to $e^{2z/a}$ for TM polarized waves.

MODE EQUATION

The prototype waveguide model considered here consists of two plates of infinite extent, parallel to the x-y plane and located at $z = 0$ and $z = h$. The interior of the guide is assumed to be free space. This prototype waveguide corresponds to the "fictitious free space region" to be later discussed in this section, where it is used to determine modal excitation factors and polarization coupling. The electromagnetic field is assumed to be independent of the y-coordinate and propagation is assumed to be in the x-direction. Any given waveguide mode is considered to be composed of two crossing plane waves, upgoing and downgoing, with wave normals at the angles $\pm\theta$ to the x-axis.

The nature of the boundary planes will be specified in terms of reflection coefficients. These coefficients are defined in terms of the ratios of specific components of the upgoing and downgoing waves and are therefore dependent on the polarization of the waves. A convenient way of describing the polarization is in terms of the linear components of the complex electric vector which are perpendicular and parallel to the plane of incidence (the x-z plane). The notation $\parallel(\perp)$ will indicate that the electric vector is parallel (perpendicular) to the plane of incidence.

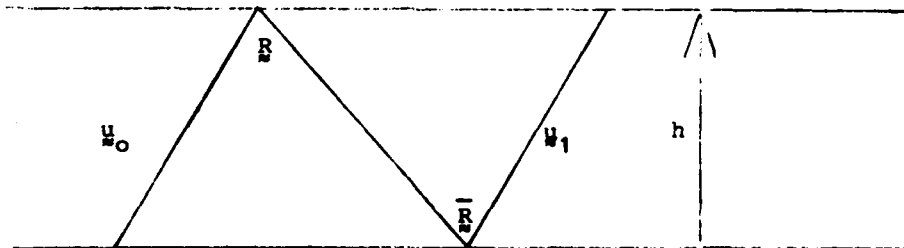
In general, the upper boundary must be considered anisotropic. Thus there can be a change in polarization upon reflection. The reflecting properties of the upper boundary are given by reflection coefficients having the matrix form

$$\underline{R} = \begin{pmatrix} \underline{R}_{11} & \underline{R}_{12} \\ \underline{R}_{21} & \underline{R}_{22} \end{pmatrix}, \quad (10)$$

where the first subscript describes the polarization of the incident (upgoing) wave and the second subscript denotes the polarization of the reflected wave. The properties of the lower boundary are assumed isotropic and specified by a diagonal reflection matrix of the form

$$\underline{\bar{R}} = \begin{pmatrix} \underline{\bar{R}}_{11} & 0 \\ 0 & \underline{\bar{R}}_{22} \end{pmatrix}. \quad (11)$$

If the upgoing wave is considered as the primary or incident wave, the downgoing wave can be considered as resulting from reflection at the upper boundary. This wave will in turn be reflected at the lower boundary, giving rise to another upgoing wave. The requirement that the second upgoing wave be the same as the original yields the mode condition. This process is shown in the diagram below.



The primary wave is represented by the column matrix \underline{u}_0 . The second upgoing wave (\underline{u}_1) is therefore given by the relationship

$$\underline{u}_1 = \underline{\bar{R}} \underline{R} \underline{u}_0 \exp[-2ikhsin(\theta)],$$

where the exponential term accounts for phase change in the double passage across the guide. The self-consistency requirement for the waveguide mode is thus

$$\det \left[\bar{R} R \exp[-2ikh \sin(\theta)] - \mathbf{1} \right] = 0, \quad (12)$$

where $\mathbf{1}$ is the unit diagonal matrix.

POINT SOURCES AND LINE SOURCES

The source is assumed to be a vertical Hertzian dipole. Budden (1961, 1962) has shown that a vertical dipole is equivalent to an infinite set of line quadrupoles, where the line quadrupoles are located parallel to the x-y plane and inclined at (complex) angles to the y-axis. This is easily seen by considering the Hertz vector for a dipole at the origin. If the dipole is parallel to the z-axis, the Hertz vector has only a z-component and is proportional to $\exp(-ikr)/r$. For a dipole of unit strength, the Hertz vector is as follows (Budden, 1962):

$$\frac{e^{-ikr}}{4\pi r} = -\frac{k}{8\pi} \int_{-\pi/2-i\infty}^{\pi/2+i\infty} \cos(\alpha) H_1^{(2)}(ks) \, d\omega, \quad (13)$$

where

$$\begin{aligned} \alpha &= \arctan \left\{ z / [x \cos(\omega) + y \sin(\omega)] \right\} \\ s &= \left\{ [x \cos(\omega) + y \sin(\omega)]^2 + z^2 \right\}^{1/2}. \end{aligned} \quad (14)$$

Thus s is the distance from a point (x, y, z) to a line in the x-y plane passing through the origin at an angle ω to the y-axis, and α is the angle between the x-y plane and the line along s . $H_1^{(2)}$ is a Hankel function of the

second kind, of order one. The term $\cos(\alpha)H_1^{(2)}(ks)$ would result from a line quadrupole source in the x-y plane at an angle ω to the y-axis. Consider a line quadrupole source as composed of two line dipole sources at $x = \frac{1}{2} \delta x$ and $x = -\frac{1}{2} \delta x$ in the x-y plane. The line dipoles consist of closely spaced dipoles oriented parallel or antiparallel to the z-axis and distributed parallel to the y-axis. The Hertz vector for the line dipoles is proportional to $H_0^{(2)}(k\rho)$ where $\rho = (x^2 + z^2)^{1/2}$. Letting δx tend to zero and letting the strengths (M, -M) of the line dipoles increase in such a way that the product $M\delta x$ remains finite will result in a term proportional to $\partial H_0^{(2)}(k\rho)/\partial x$, which reduces to a term of the form $\cos(\theta)H_1^{(2)}(k\rho)$, where $\cos(\theta) = x/\rho$. From the definitions of s and α in (14), it is clear that the integral in (13) results from an infinite set of line quadrupoles in the x-y plane, each at a different angle ω to the y-axis. Because the path of integration in (13) is not unique, there is an infinite number of ways in which the angles ω may be chosen.

Consider a guide bounded by perfectly conducting plates with a line source parallel to the y-axis. This source generates waveguide modes, and each consists of crossing plane waves with normals in the x-y plane at angles $\pm\theta_m$ to the x-axis. For a line source at an angle ω to the y-axis, the component plane wave has the form $\exp(-ik\{[x \cos(\omega) + y \sin(\omega)]C_m + z S_m\})$, where $C_m = \cos(\theta_m)$ and $S_m = \sin(\theta_m)$. A point source within the guide is now represented by an infinite set of line sources such that the total field of the component wave is proportional to

$$\int_{-\pi/2-i\infty}^{\pi/2+i\infty} \exp(-ik\{[x \cos(\omega) + y \sin(\omega)]C_m + z S_m\}) d\omega . \quad (15)$$

Making the substitutions $\rho = (x^2 + y^2)^{1/2}$ and $\cos(u) = x/\rho$ in (15),

$$\int_{-\pi/2-i\infty}^{\pi/2+i\infty} \exp(-ik\rho C_m \cos(\omega-u)) \exp(-ikz S_m) d\omega . \quad (16)$$

The integration in (16) yields a Hankel function of the second kind, of order zero (Sommerfeld, 1949). Thus the total field of the component wave is proportional to

$$H_0^{(2)}(k\rho C_m) \exp(-ikzS_m).$$

The appropriate Hankel function exchange for the exponential term when a line source is used is therefore

$$\exp(-ikxC_m) + H_0^{(2)}(k\rho C_m). \quad (17)$$

MODAL EXCITATION FACTORS AND POLARIZATION COUPLING

The excitation of waveguide modes is conveniently treated in terms of line sources. The technique consists of selecting one of the possible line sources for the integrand in (13), finding the mode excitation for this line source, then effecting a change from an exponential term to the appropriate Hankel function. Following the method of Budden (1961, 1962), the source is a line of quadrupoles at height d (near the ground) parallel to the y -axis. A fictitious free space region is introduced that extends from $z = l$ (lower) to $z = u$ (upper) such that $l < d < u$ (the line source is assumed within the free space region). The region above $z = u$ is characterized by the reflection coefficient matrix R_u , while the region below $z = l$ is characterized by a reflection coefficient matrix \bar{R}_l . If the line source has unit strength, the y -component of the magnetic field in infinite free space can be written

$$H_y = \frac{k_0^3}{4\pi\epsilon_0} \int_{0-i\infty}^{\pi+i\infty} \exp(ik_0(xC + |z-d|S)) C^2 d\theta, \quad (18)$$

where $C = \cos(\theta)$, $S = \sin(\theta)$, and the limits of integration are selected to ensure convergence for all x (Sommerfeld, 1949). The primary field integrand in equation (18) represents a plane wave which undergoes reflections at $z = u$ and $z = l$, and these reflected waves must be added to the primary field to obtain the total field. Four combinations are possible, two from waves

initially upgoing or downgoing at the source and two from waves reaching the reception point upgoing or downgoing.

An initially upgoing wave is converted to a downgoing wave by the reflection process denoted by the operator $(R_u \bar{R}_1)^N \bar{R}_u$ and to an upgoing wave by the operator $(\bar{R}_1 R_u)^N$. An initially downgoing wave is converted to an upgoing wave by the operator $(\bar{R}_1 R_u)^N \bar{R}_1$ and to a downgoing wave by the operator $(R_u \bar{R}_1)^N$. The N denotes N reflection processes of the type described by the bracketed term. With each reflection process must also be associated phase terms to account for the transversals to and fro between $z = l$ and $z = u$. The subscripts u and l denote reflection coefficients evaluated at $z = u$ and $z = l$, respectively.

The total field is obtained by combining the primary and all reflected fields and letting the dimensions of the free space region tend to zero. This requires taking the limits $l \rightarrow u$ and $z \rightarrow d$ in such a way that $l < d < u$ is maintained. The total field may be written as

$$\begin{aligned}
 H_y = & \frac{k_o^3}{4\pi\epsilon_o} \sum_{N=0}^{\infty} \int e^{-ik_o xC} (R_u \bar{R}_1)^N \bar{R}_u c^2 d\theta \\
 & + \frac{k_o^3}{4\pi\epsilon_o} \sum_{N=0}^{\infty} \int e^{-ik_o xC} (\bar{R}_1 R_u)^N \bar{R}_1 c^2 d\theta \\
 & + \frac{k_o^3}{4\pi\epsilon_o} \sum_{N=1}^{\infty} \int e^{-ik_o xC} (R_u \bar{R}_1)^N \bar{R}_u c^2 d\theta \\
 & + \frac{k_o^3}{4\pi\epsilon_o} \sum_{N=1}^{\infty} \int e^{-ik_o xC} (\bar{R}_1 R_u)^N \bar{R}_1 c^2 d\theta .
 \end{aligned} \tag{19}$$

The reflection coefficients are evaluated at $z = d$ and the subscripts l and u are no longer needed. In equation (19), the first summation starts with $N=0$ in order to include the primary, nonreflected wave; and \underline{p} is a column matrix whose second element is zero, corresponding to a vertical electric dipole source.

The order of summation and integration is now reversed so that each integrand will contain a geometric series. It can be shown (Budden, 1961, 1962) that the series converges for certain simplified cases, and convergence is assumed here. Summation of the geometrical series gives

$$\sum_{N=0}^{\infty} (\bar{R} \underline{R})^N = (\underline{1} - \bar{R} \underline{R})^{-1} \quad (20)$$

$$\begin{aligned} \sum_{N=1}^{\infty} (\bar{R} \underline{R})^N &= (\bar{R} \underline{R}) (\underline{1} - \bar{R} \underline{R})^{-1} \\ &= \bar{R} (\underline{1} - \bar{R} \underline{R})^{-1} \underline{R} \end{aligned} \quad (21)$$

$$\begin{aligned} \sum_{N=1}^{\infty} (\bar{R} \underline{R})^N \underline{R} &= (\underline{R})^{-1} \sum_{N=1}^{\infty} (\bar{R} \underline{R})^N \\ &= \underline{R} (\underline{1} - \bar{R} \underline{R})^{-1}. \end{aligned} \quad (22)$$

Consequently the result of summing the series in equation (19) is

$$H_y = \frac{k_o^3}{4\pi\epsilon_o} \int_{0-i\infty}^{\pi+i\infty} e^{-ik_o xC} (\underline{1} + \underline{R}) (\underline{1} - \bar{R} \underline{R})^{-1} (\underline{1} + \bar{R}) \underline{p} c^2 d\theta. \quad (23)$$

If the sign of θ is reversed, the role of incident and reflected wave is exchanged and each reflection element is replaced by its inverse. The integrand simply changes sign upon reversal of the sign of θ . The integral may be evaluated by using the theory of residues, deforming the contour to run symmetrically through the origin from $\pi/2 + i\infty$ to $-\pi/2 - i\infty$. Because the integrand is antisymmetric about $\theta = 0$, the integral along the new contour is zero. In changing the contour, however, singularities are crossed. The most important of these are poles of the factor $(\mathbf{1} - \bar{\mathbf{R}} \mathbf{R})^{-1}$. The residue contribution of a simple pole at θ_n is as follows:

$$H_{yn} = \frac{ik_0^3}{2\epsilon_0} e^{-ik_0 x C_n} \frac{(\mathbf{1} + \mathbf{R})_n X_n (\mathbf{1} + \bar{\mathbf{R}})_n \mathbf{R} C_n^2}{\left(\frac{\partial F}{\partial \theta}\right)_{\theta_n}} \quad (24)$$

where

$$F = \det (\mathbf{1} - \bar{\mathbf{R}} \mathbf{R}) \quad (25)$$

$$X_n = \lim_{\theta \rightarrow \theta_n} [F(\mathbf{1} - \bar{\mathbf{R}} \mathbf{R})^{-1}],$$

and the subscript, n , signifies that the quantities are evaluated at $\theta = \theta_n$. The pole condition $F = 0$ is identical to the waveguide mode equation (12) in the limit $h \rightarrow 0$. Thus the solution of the pole condition yields the waveguide modes, and the residues at the poles give the excitation factors. Performing the matrix multiplications in equation (24), using the Hankel function substitution [equation (17)], and employing the geometrical spreading factor yields the equation

$$H_{yn} = \frac{-k_0^{5/2} C_n^{3/2} e^{i\frac{\pi}{4}}}{2\epsilon_0 \sqrt{2\pi a} \sin(\rho/a)} \frac{(1 + \bar{R}_1)^2 (1 - \bar{R}_{11} R_1)}{\bar{R}_1 \left(\frac{\partial F}{\partial \theta}\right)_{\theta_n}} e^{-ik_0 \rho C_n} \quad (26)$$

To be compatible with the mode sum of Section 1 [equation (1)], it is necessary to change the reference direction for θ from the x-axis to the z-axis. Doing so simply requires interchanging the factors S and $\sin(\theta)$ with the factors C and $\cos(\theta)$.

Equation (26) requires the source and reception point to be at the same height, which is also the height at which the reflection elements are to be determined. If the dependence of H_{yn} on height z is given by the function $G_n(z)$, then an obvious extension of equation (26) to include arbitrary source and reception height involves multiplication by the function

$$\frac{G_n(z_T)}{G_n(d)} \frac{G_n(z_R)}{G_n(d)},$$

where z_T is the transmitter height, z_R is the receiver height, and d is the evaluation height for the reflection elements, assumed to be below the ionosphere.

Whenever the ionosphere is assumed to be isotropic (no geomagnetic field), the field components can be divided into two sets. These are the well-known TE ($H_y = 0$) and TM ($E_y = 0$) modes. When anisotropy is included, however, a given mode, in general, involves both H_y and E_y . To determine the coupling between the TM and TE components of the eigenfunctions, we again introduce a thin fictitious region of free space within the transformed planar waveguide. The region is assumed to be centered at some altitude $z = d$ which is below the ionosphere, so that the region $z < d$ can be considered isotropic. Within this region, the fields of the TM and TE components can be considered in terms of upgoing and downgoing plane waves. Furthermore, the eigenfunctions satisfy the condition that a particular component, say the upgoing, must be returned to its original value after being reflected from the two boundaries of the thin free space region. Thus, for the upgoing component e_1^u (the component perpendicular to the plane of propagation), the requirement is that

$$e_{\perp}^u = \frac{\bar{R}_{\perp}}{1 - \bar{R}_{\perp} R_{\perp}} e_{\perp}^u + \frac{\bar{R}_{\perp}}{1 - \bar{R}_{\perp} R_{\perp}} e_{\perp}^u$$

or

$$\frac{e_{\perp}^u}{e_{\perp}^u} = \frac{1 - \bar{R}_{\perp} R_{\perp}}{\bar{R}_{\perp} R_{\perp}} \quad (27)$$

In the free space region

$$e_{\perp}^u = \cos(\theta) e_x^u - \sin(\theta) e_z^u \equiv h_y^u$$

$$e_{\perp}^u = e_y^u,$$

where h_y^u is the upgoing component of H_y and e_y^u is the upgoing component of E_y . The total H_y and E_y fields within the free space gap at $z = d$ are therefore represented by the equations

$$E_y = e^{-ik_0 Cd} \left(1 + \frac{1}{\bar{R}_{\perp}} \right)$$

$$H_y = \left(\frac{1 - \bar{R}_{\perp} R_{\perp}}{\bar{R}_{\perp} R_{\perp}} \right) \left(1 + \frac{1}{\bar{R}_{\perp}} \right) e^{-ik_0 Cd},$$

and their ratio is as follows:

$$\frac{E_y(d)}{H_y(d)} = \frac{\bar{R}_{\perp} R_{\perp} (1 + \bar{R}_{\perp})}{(1 - \bar{R}_{\perp} R_{\perp})(1 + \bar{R}_{\perp})} \equiv \gamma(d) \quad (28)$$

In equation (28) the reflection coefficients are evaluated at $z = d$.

3. WAVEGUIDE MODE THEORY - HORIZONTALLY INHOMOGENEOUS GUIDES

If significant variations occur (as they often do) along the direction of propagation in the earth-ionosphere waveguide, then homogeneous guide formulations require modification. For such cases, there are two techniques for mode summation that are commonly used at VLF. One employs a WKB approach; the other uses mode conversion.

In the WKB technique, an eigenmode is assumed to be uniquely and independently identifiable anywhere along a propagation path. Furthermore, each mode is assumed to depend only on the local characteristics of the waveguide and to propagate independently of the existence of any other modes. The WKB formulation generalizes the expression for the mode summation in equation (1) to the form

$$E_v(d) = \frac{K(P, f)}{\sqrt{\sin d/a}} \sum_n (\Lambda_n^T \Lambda_n^R)^{1/2} G_{nGn}^{TR} e^{-ik_0 \int_0^d S_n(x) dx} \quad (29)$$

Note that the only differences arise from (1) the use of the geometric mean of the excitation factors at transmitter (Λ_n^T) and from receiver (Λ_n^R) locations and (2) the integration of the complex propagation factor along the path. The WKB formulation was apparently introduced simply as an "obvious extension" of the homogeneous mode sum by Wait (1964), who further noted that the form is similar to what would be expected if a WKB formulation were applied, although no actual derivation was presented. The use of the name WKB mode sum has persisted.

In the mode conversion method, eigenmodes are assumed to be uniquely and independently identified only in a local sense. Even though the eigen characteristics of a mode depend only on local characteristics of the waveguide, the propagation of each mode depends not only on the existence of other modes but also on the past and future propagation history of itself and the other modes.

The approach that uses mode conversion does not lend itself conveniently to consideration of transition fading on very long VLF propagation paths. The WKB method, although easily applied, is unable to handle the rapid change in guide characteristics that occurs at the terminator (Pappert and Snyder, 1972). A difficulty encountered when using mode conversion arises from the necessity of knowing the future propagation history of each mode. Making appropriate assumptions to relieve this requirement can lead to some simplification, but the resulting formulation is still not convenient for very long paths. A further difficulty is that conventional mode conversion techniques require a knowledge of all the vector components of the electromagnetic field throughout all space.

Numerous methods have been presented for circumventing the latter problem. Wait (1968a, b), for example, formulated mode conversion by using isotropic impedance boundary conditions, with the result that fields were required only for the region between the upper (ionospheric) and the lower (ground) impedance boundaries. Such boundary conditions are certainly not appropriate for the nighttime ionosphere and thus for consideration of transitions from night to day. Smith (1974) extended Wait's (1968a, b) results to include boundary anisotropy by using impedance matrix boundary conditions. His analysis however, was for a planar, empty waveguide and was directed toward considering ground effects.

Galejs (1971) presented a modified mode conversion formulation for an abrupt change between daytime and nighttime anisotropic ionospheres. Conventional mode conversion theory usually represents the EM field as an expansion in terms of a suitably chosen complete set of orthogonal functions. The Galejs formulation employs an incomplete set of nonorthogonal functions. The formulation now to be employed is similar to that of Galejs (1971).

OPERATOR EQUATIONS

The operator equations presented in this section are based on Maxwell's equations in two (rectangular) dimensions and are patterned after the formulations of Pappert and Smith (1972). Furthermore, material media are assumed to be characterized by constitutive parameters (permittivity and permeability) that can be inhomogeneous in one dimension. This is quite compatible with the usual procedure for handling the earth-ionosphere waveguide by describing the

electromagnetic properties of the ionosphere with the aid of a vertically inhomogeneous dielectric tensor.

We start with equation (5), use the substitutions in equation (6), and eliminate the E_x and H_x components. This leads to the differential operator equation

$$\underline{L} \underline{e} = -\frac{1}{ik_0} \frac{\partial \underline{e}}{\partial x}, \quad (30)$$

where \underline{e} is a four-element column vector:

$$\underline{e} = \begin{pmatrix} E_Y \\ E_Z \\ H_Y \\ H_Z \end{pmatrix}, \quad (31)$$

and \underline{L} is a 4 x 4 matrix differential operator. Equation (30) is cast as an eigenvalue equation by using the functional form $\exp[-ik_0 S_n x]$, so that $\underline{L} \underline{e}_n = S_n \underline{e}_n$. These \underline{e}_n form the set of expansion functions used in conventional mode conversion theory.

To find an operator adjoint to \underline{L} , a procedure discussed by Pappert and Smith (1972) is used. First, let the inner product be defined:

$$\langle \underline{a}, \underline{b} \rangle = \int_{-\infty}^{\infty} \tilde{\underline{a}}^* \cdot \underline{b} \, dz, \quad (32)$$

where the tilde over \underline{a} denotes transpose and the asterisk denotes conjugation. Next, the operator adjoint to \underline{L} is defined by the relationship

$$\langle \underline{L}^+ \underline{w}, \underline{e} \rangle = \langle \underline{w}, \underline{L} \underline{e} \rangle, \quad (33)$$

which is just a prescription for integration by parts to find the form of I_n^+ as well as the necessary boundary conditions on the adjoint functions (w) in order that the integrated contributions vanish. Pappert and Smith (1972) showed that the adjoint functions can be obtained from direct functions by considering a second waveguide which is related to the original one in a simple way. In the original guide, the z-axis is taken as vertical and propagation is assumed in the xz-plane. The x-direction-cosine of the geomagnetic field is l in the original guide. The adjoint guide is obtained by replacing l with $-l$. By examining symmetry properties of the elements of the ionospheric permittivity tensor, Pappert and Smith (1972) showed that the adjoint eigenfunctions are given in terms of eigenfunctions of the adjoint waveguide according to the relationship

$$\tilde{w}_n^* = \begin{pmatrix} w_{1n}^* \\ w_{2n}^* \\ w_{3n}^* \\ w_{4n}^* \end{pmatrix} = \begin{pmatrix} H_{zn}(-l) \\ -H_{yn}(-l) \\ -E_{zn}(-l) \\ E_{yn}(-l) \end{pmatrix}. \quad (34)$$

Further, from the definition of adjoint given by equation (33) the usual biorthogonality relations hold. Thus

$$\begin{aligned} \langle I_n^+ \tilde{w}_n, e_m \rangle &= \lambda_n^* \langle \tilde{w}_n, e_m \rangle \\ &= \langle \tilde{w}_n, l e_m \rangle \\ &= S_m \langle \tilde{w}_n, e_m \rangle, \end{aligned}$$

which shows both that $\langle \tilde{w}_n, e_m \rangle = 0$ and that $\lambda_n = S_n^*$ for nondegenerate eigenfunctions.

MODE CONVERSION

Fundamental to the mode conversion formulation employed here is the notion that any variation in the VLF propagation conditions along a path can

be modeled as a series of discrete changes between homogeneous sections along the path. With this in mind, it is seen that the fundamental analytical requirement is the determination of mode conversion coefficients due to a single abrupt change in waveguide characteristics.

Following classical procedures, consider a mode of unit amplitude incident on such a discontinuity in a waveguide. This mode is described in terms of its height-gain function, $\vec{e}_j^+{}^I(z)$, where the superscript I denotes the incident region, the subscript j denotes the jth mode, the overarrow indicates a forward-propagating mode, and the undertilde indicates a vector quantity. Note that the terms height-gain function and eigenfunction are used here interchangeably even though more traditional usage limits the term height-gain to individual components of the vector eigenfunction. The discontinuity in the guide generates both reflected, or backward-propagating, modes within the incident region (I) and transmitted, or forward-propagating, modes within the transmission region (II). Backward-propagating modes might also exist in region II due to another discontinuity; these will therefore be included. The continuity requirements lead to the equation

$$\vec{e}_j^+{}^I(z) + \sum_m r_{mj} \vec{e}_m^+{}^I(z) = \sum_n T_{nj} \vec{e}_n^+{}^{II}(z) + \sum_l R_{lj} \vec{e}_l^+{}^{II}(z), \quad (35)$$

which is independent of the position of the discontinuity between regions I and II. In equation (35), r_{mj} is a coefficient describing the conversion of the incident mode (j) into a backward-traveling mode (m) in region I $[\vec{e}_m^+{}^I(z)]$, and T_{nj} is a coefficient describing conversion of the incident mode (j) into the forward traveling mode (n) of region II $[\vec{e}_n^+{}^{II}(z)]$. The R_{lj} are the coefficients appropriate to possible backward-traveling modes in region II $[\vec{e}_l^+{}^{II}(z)]$.

Recall that a major problem with implementation of mode conversion concepts arises from the need to know the future propagation history. In terms of equation (35), this concept is represented by the coefficients R_{lj} . By making the assumption that appreciable reflection does not occur, so that there can be no backward-traveling modes, the R_{lj} may be set equal to zero. The r_{mj} are then also all zero, and equation (35) reduces to

$$\mathcal{E}_j^{\text{+I}}(z) = \sum_n T_{nj} \mathcal{E}_n^{\text{+II}}(z). \quad (36)$$

The assumption of negligible reflection is not unique to this study. It is commonly made and has been demonstrated to be adequate in numerous cases (Wait, 1968a, b; Galejs, 1971; Pappert and Snyder, 1972; Smith, 1974). In equation (36), there are assumed to be N modes in region II, so that there are N conversion coefficients.

Conventional mode conversion techniques require multiplication of equation (36) by the transpose conjugate of the adjoint function for the mth forward-traveling mode in region II, followed by integration over all space. Doing so, and recalling the biorthogonality relationships, we obtain the well-known result

$$\int_{-\infty}^{\infty} \tilde{w}_m^* \cdot \mathcal{E}_j^{\text{+I}} dz = T_{mj} \int_{-\infty}^{\infty} \tilde{w}_m^* \cdot \mathcal{E}_m^{\text{+II}} dz,$$

more conveniently written as

$$I_{m,j}^{\text{II,I}} = T_{mj} I_{m,m}^{\text{II,II}} \quad (m = 1, N). \quad (37)$$

Solving for the conversion coefficient yields the apparently simple result

$$T_{mj} = I_{m,j}^{\text{II,I}} / I_{m,m}^{\text{II,II}}. \quad (38)$$

The simplicity of equation (37) depends on knowing the height-gain functions throughout all space. Such a requirement is the main limitation to the application of mode conversion techniques to very long VLF paths. Relaxing the integration limits to some finite value prevents use of the biorthogonality relationships and yields, instead of equation (37), the result

$$I_{m,j}^{II,I} = \sum_n T_{nj} I_{m,n}^{II,II} \quad (m = 1, N), \quad (39)$$

where there are N equations and N unknowns, so that the system can be solved for the T_{nj} . In equation (39),

$$\begin{aligned} I_{m,j}^{II,I} &= \int_{-\infty}^h \tilde{w}_m^{*II} \cdot \tilde{e}_j^I dz \\ I_{m,n}^{II,II} &= \int_{-\infty}^h \tilde{w}_m^{*II} \cdot \tilde{e}_n^{II} dz, \end{aligned} \quad (40)$$

where the overarrow notation is dropped because only forward-propagating modes are considered.

For application to the VLF earth-ionosphere problem, the above procedure may be justified as follows. First, the various eigenvalues and eigenfunctions are determined by using the complete geometry ($-\infty < z < +\infty$). Second, the eigenfunctions can be expected to decay rapidly within the earth and within the ionosphere. Below the ionosphere but within the waveguide, the vector eigenfunctions degenerate into the isotropic TM and TE components, with a prescribed coupling between the two for a given mode. By taking the upper limit on the integral to be within the guide and below the ionosphere, it is possible to write the various integrals, $I_{n,k}$, in terms of known functions—namely the modified Hankel functions, as defined by the Computation Laboratory Staff at Cambridge, Massachusetts (1945). The procedure used here is actually expansion in terms of "nonorthogonal" functions and is certainly better than assuming orthogonality and "throwing away" the contributions to the integrals from the ionosphere.

The j th vector eigenfunction for either region is defined to be [from equation (31)]

$$\tilde{e}_j = \begin{pmatrix} e_{y1} \\ e_{zj} \\ h_{yj} \\ h_{zj} \end{pmatrix}. \quad (41)$$

Because the upper limit on the integrals in equation (40) is to be taken below the ionosphere, equation (41) can be written as

$$\underline{e}_j = \begin{pmatrix} e_{yj} \\ -S_j h_{yj} \\ h_{yj} \\ S_j e_{yj} \end{pmatrix}.$$

The adjoint vector eigenfunction is given by equation (34) as

$$\underline{w}_m = \begin{pmatrix} h_{zm}^* (-l) \\ -h_{ym}^* (-l) \\ -e_{zm}^* (-l) \\ e_{ym}^* (-l) \end{pmatrix} = \begin{pmatrix} S_m^* e_{ym}^* (-l) \\ -h_{ym}^* (-l) \\ S_m^* h_{ym}^* (-l) \\ e_{ym}^* (-l) \end{pmatrix},$$

where the notation indicates that elements of the adjoint eigenfunction are obtained by reversing the x-axis direction-cosine of the earth's biasing magnetic field. The first integral in equation (40) thus becomes

$$I_{m,j}^{II,I} = (S_m^{II} + S_j^I) \int_0^h [e_{ym}^{II}(-l) e_{yj}^I + h_{ym}^{II}(-l) h_{yj}^I] dz. \quad (42)$$

The normalization of the eigenfunctions is such that $h_{ym}(-l) = h_{ym}$. However, from equation (28)

$$\frac{e_y(-l)}{e_y} = \frac{Y(d, -l)}{Y(d)} = \frac{R_1(-l)(1 - \bar{R}_1 R_1)}{R_1(1 - \bar{R}_1 R_1(-l))}. \quad (43)$$

Because ${}_1R_1(-l) = {}_1R_1$ and ${}_1R_1(-l) = {}_1R_1$ (Budden, 1961b), equation (43) becomes

$$\frac{e_y(-l)}{e_y} = \frac{{}_1R_1}{{}_1R_1}.$$

Denoting this ratio as A_m , equation (42) becomes

$$I_{m,j}^{II,I} = (S_m^{II} + S_j^I) \int_0^h [A_m e_{ym}^{II} e_{yj}^I + h_{ym}^{II} h_{yj}^I] dz. \quad (44)$$

The integrals in equation (44) are now easily evaluated by using the conventional "multiply and subtract" method. In this method, we multiply the differential equation for the height-gain of mode m by the height-gain of mode n and the differential equation for the height-gain of mode n by the height-gain of mode m and subtract. The differential forms are obtained from equation (9a, b) and will be presented shortly [see equation (50)]. Performing the multiplication and subtraction for h_y components leads to

$$h_{ym} \frac{d^2 h_{yn}}{dz^2} - h_{yn} \frac{d^2 h_{ym}}{dz^2} - k_o^2 (c_m^2 - c_n^2) h_{ym} h_{yn} = 0,$$

or

$$\frac{d}{dz} \left(h_{ym} \frac{dh_{yn}}{dz} - h_{yn} \frac{dh_{ym}}{dz} \right) = k_o^2 (c_m^2 - c_n^2) h_{ym} h_{yn}.$$

The second integral in equation (44) thus becomes

$$\int_0^h h_{ym}^{II} h_{yj}^I dz = \frac{h_{ym}^{II} \frac{dh_{yj}^I}{dz} - h_{yj}^I \frac{dh_{ym}^{II}}{dz}}{k_0^2 (c_m^{II} - c_j^I) (c_m^{II} + c_j^I)} \Big|_0^h$$

$$= \frac{-i [h_{ym}^{II} e_{xj}^I - h_{yj}^I e_{xm}^{II}] h}{k_0^2 (c_m^{II} - c_j^I) (c_m^{II} + c_j^I)} \Big|_0^h, \quad (45)$$

while the first integral in equation (44) is

$$\int_0^h e_{ym}^{II} e_{yj}^I dz = \frac{i [e_{ym}^{II} h_{xj}^I - e_{yj}^I h_{xm}^{II}] h}{k_0^2 (c_m^{II} - c_j^I) (c_m^{II} + c_j^I)} \Big|_0^h. \quad (46)$$

In equations (45) and (46), it is assumed that $c_m^{II} \neq c_j^I$ for all m and j . Evaluation of the second integral in equation (40) proceeds in the same manner. The only difference is the fact that all field components in this case pertain to region II of the waveguide. In this case however, the situation $m = j$ results in division by zero in equations (45) and (46), and special treatment is required. For the case $m = j$ in region II, the use of L'Hospital's rule yields

$$\int_0^h h_{yj}^2 dz = \frac{1}{\alpha} [(c_j^2 + \alpha z) h_{yj}^2 - e_{xj}^2] h \Big|_0^h \quad (47)$$

$$\int_0^h e_{yj}^2 dz = \frac{1}{\alpha} [(c_j^2 + \alpha z) e_{yj}^2 - h_{xj}^2] h \Big|_0^h, \quad (48)$$

where the superscript "II" is omitted.

The contribution to the integral in equation (40) due to the fields in the ground is obtained as follows. The fields vary as $\exp(+ik_0 z)$ in the ground, which gives

$$\int_{-\infty}^0 h_{yj}^I h_{ym}^{II} dz = - \frac{i}{k_0 (\tau_j^I + \tau_m^{II})}$$

$$\int_{-\infty}^0 e_{yj}^I e_{ym}^{II} dz = \frac{i \gamma_j^I \gamma_m^{II}}{k_0 (\tau_j^I + \tau_m^{II})} . \quad (49)$$

The individual height-gains are obtained in the following way. Consider the transformed planar guide already discussed under Coordinate Transformation. In order to be compatible with the assumptions discussed under Mode Equation and under Mode Excitation Factors and Polarization Coupling, the waveguide region is assumed to be filled with the "equivalent" permeability or dielectric medium as described in under Coordinate Transformation. The fields within the "filled" region satisfy equations (9a, b) while the fields within the earth have simple exponential forms.

Since all altitudes of interest are small compared to the radius of the earth (a), the exponential term in equation (9) is expanded to first order in z/a. A variation in the x-direction of the form $e^{-ik_0 Sx}$ is assumed. Note that the variable S will be identified later as $\sin(\theta)$, where the angle θ is referenced to the vertical rather than to the horizontal as in previous sections. With the above assumptions, equation (9b) for TM waves becomes

$$H_y'' + k_0^2 (C^2 + \alpha z) H_y = 0, \quad (50)$$

where $C^2 = 1-S^2$, $\alpha = 2/a$, and the double prime denotes second differentiation with respect to z.

With the change of variable

$$t = \frac{k_0}{a} (c^2 + az)^{2/3}, \quad (51)$$

the equation becomes

$$H_y'' + tH_y = 0, \quad (52)$$

where now the double prime denotes differentiation with respect to t . Equation (52) is Stokes' equation. Thus, H_y is linearly expressible in terms of solutions to Stokes' equation. In this study, we shall use the modified Hankel functions of order one-third (h_1, h_2), as defined by the Computation Laboratory Staff at Cambridge, Massachusetts (1945). Using a similar procedure for TE polarization, we shall arrive at similar results except that the transformed planar guide will contain a medium with refractive index given by $e^{z/a}$.

The waves in the two regions are given by the following relationships:

$$\text{Region I: } H_y = a_1 h_1(t) + a_2 h_2(t) \\ z > d$$

$$E_x = i \left[\frac{a}{k_0} \right]^{1/3} [a_1 h_1'(t) + a_2 h_2'(t)]$$

$$\text{Region II: } H_y = e^{ik_0 \tau z} \\ z > 0$$

$$E_x = -\frac{\tau}{N^2} e^{ik_0 \tau z}$$

where h_1 and h_2 are modified Hankel functions of order one-third, N is the refractive index of the ground, and $\tau = (N^2 - S^2)^{1/2}$, taken with negative imaginary part. Continuity requirements between the regions leads to the results

$$H_y = f_1(z) ,$$

where

$$f_1(z) = H_2(t_0) h_1(t_z) - H_1(t_0) h_2(t_z)$$

$$H_j(t_z) = h_j'(t_z) - i \left[\frac{k_0}{a} \right]^{1/3} \frac{\tau}{N^2} h_j(t_z)$$

$$t_z = \left[\frac{k_0}{a} \right]^{2/3} (c^2 + az) \quad (53)$$

Following a similar procedure, results for the TE polarization are given:

$$E_y = f_1(z),$$

where

$$f_1(z) = F_2(t_0) h_1(t_z) - F_1(t_0) h_2(t_z)$$

$$F_j(t_z) = h_j'(t_z) - i \left[\frac{k_0}{a} \right]^{1/3} \tau h_j(t_z).$$

(54)

Normalizing the H_y component to 1 at $z = 0$ and using equation (28) for the polarization coupling, we arrive at the final forms for the height gains:

$$h_y(z) = \frac{f_I(z)}{f_I(0)} \quad (55a)$$

$$e_y(z) = Y(d) \frac{f_I(d) f_I(z)}{f_I(0) f_I(d)} \quad (55b)$$

$$e_x(z) = i \frac{\alpha}{k_0} \frac{1}{3} \frac{1}{f_I(0)} \frac{df_I(z)}{dz} \quad (55c)$$

$$h_x(z) = -i \frac{\alpha}{k_0} \frac{1}{3} \frac{\rho(d) f_I(d)}{f_I(0) f_I(d)} \frac{df_I(z)}{dz} \quad (55d)$$

$$e_z(z) = -Sh_y(z) \quad (55e)$$

$$h_z(z) = SY(d)h_y(z). \quad (55f)$$

Once the conversion coefficients are obtained, it is necessary to sum over all the incident modes. This requires evaluation of the amplitudes of the incident modes. This can be done by starting at the transmitter, where the modal excitation factors give the mode amplitudes, and by assuming that the regions between the discontinuities are homogeneous.

Notationally this can be written as

$$\underline{A}^I = \underline{P}^I \underline{A}^I, \quad (56)$$

where the equation

$$\underline{A}^I = \begin{pmatrix} A_1^I \\ \vdots \\ A_j^I \end{pmatrix}$$

represents the amplitudes of the incident modes (A_j^I) at the end of the region I and the equation

$$\underline{a}^I = \begin{matrix} a_1^I \\ \vdots \\ a_j^I \end{matrix}$$

represents the amplitudes of the modes at the start of region I. The factor P_n^I is a diagonal matrix with the nth diagonal element given as follows:

$$P_n^I = e^{-ik_0 S_n^I (\Delta\rho)^I} \quad (57)$$

Note that P_n^I represents the propagation factor appropriate to a homogeneous section of length $(\Delta\rho)^I$, assumed to be the length of region I. Note that the amplitudes of the modes in region II just after conversion can be conveniently written as

$$\underline{a}^{II} = \underline{T} \underline{a}^I = \underline{T} \underline{P}^I \underline{a}^I, \quad (58)$$

where \underline{T} is a rectangular matrix of the conversion coefficients from region I into region II.

A mode conversion formulation has been presented by Pappert and Shockey (1974), but important differences exist between their treatment and that employed here. Differences occur both in the numerical procedures employed and in the definition of the conversion coefficients. In the present formulation a conversion coefficient is computed at each slab interface independently of any previous conditions. In the Pappert formulation, the conversion coefficients are defined and computed in such a way that the effect of the propa-

gation factor [equation (57)] is included. Both definitions of conversion coefficients are reasonable, although their numerical values can be quite different. For example, first consider an isolated terminator specified as an abrupt transition. The two formulations will give the same results for the conversion coefficients. Next suppose that the terminator has a substantial extent. The conversion coefficients then differ for each slab interface after the first because the Pappert formulation includes the accumulated effects of propagation through the transition region, whereas the current formulation does not. In any case, the resulting mode sums computed by means of either formulation will be sensibly the same, with differences primarily due to computer numerics.

The Pappert definition of conversion coefficients is useful for studying a horizontal inhomogeneity that exists over a small distance, such as the dawn-dusk terminator. A similar conversion coefficient can be derived from the mode constants and the mode conversion coefficients presented in this study. What is required is the complex amplitude of a mode at the end of such a confined inhomogeneity resulting from a single mode of unit amplitude at the start of the inhomogeneity.

Denote by region 1 the region prior to the start of the inhomogeneity. The complex amplitudes of the modes in the first region of inhomogeneity (called region 2) due to a mode of unit amplitude and number k in region 1 are given by the conversion coefficients $T_{m,k}^{2,1}$ [see equation (44)]. The complex amplitudes of the modes at the end of region 2 are $A_{m,k}^2$, where

$$A_{m,k}^2 = P_m^2 T_{m,k}^{2,1}$$

and P_m^2 is the propagation factor for mode m in region 2 [see equation (57)]. The complex amplitude of mode n at the start of the next region (region 3) due to a mode of unit amplitude in region 2 is $T_{n,m}^{3,2}$, so that the actual complex amplitude of the mode n in region 3 is given by the product of $T_{n,m}^{3,2}$ and

. Summation over all the modes of region 2 gives the total complex

amplitude of mode n. Thus

$$a_{n,k}^3 = \sum_m A_{m,k}^2 T_{n,m}^{3,2} P_m^2 T_{m,k}^{2,1}. \quad (59)$$

This result can be generalized to any inhomogeneity along the path. We obtain

$$a_{m,k}^p = \sum_n T_{m,n}^{p,p-1} P_n^{p-1} a_{n,k}^{p-1}. \quad p > 3 \quad (60)$$

The formulations presented in this section have been implemented in a computer program written in FORTRAN. The development of the numerical calculations required for the reflection coefficients and waveguide modes has occurred over many years. These efforts have been supported by the Defense Nuclear Agency, NAVELEX PME 117, the Defense Communications Agency, and the US Coast Guard.

4. FASTMC

FASTMC is a computer program which employs the approximate mode conversion model described in section 3. The program is written in Univac's version of ASCII FORTRAN. It accepts card image input and generates plots. Additional outputs available are printouts of the amplitude and phase and binary output of the complex field. The source is an arbitrarily oriented dipole at any altitude within the waveguide. The vertical (e_z) and horizontal broadside (e_y) fields at any altitude can be obtained.

Input to the program is controlled by a set of control cards which define the type of data being read and allow standard defaults to apply. These control cards are described below. All eighty columns of these cards are read and printed. However, only the first four columns are examined by the program. Thus, the input card and the printout can contain additional comment. For example, "NAMELIST DATA FOR ELEVATED TRANSMITTER" can be used in place of the minimum requirement of "NAME". The control cards are described below, and a sample set is shown in figure 1.

NAME	Signals that NAMELIST data follow. In this program the NAMELIST name is DATUM. The NAMELIST variables are described below.
ICOMP	= Index of received electric field component = 1 gives the vertical field (Z) - DEFAULT = 2 gives the horizontal transverse field (Y)
TALT	= Transmitter altitude in km - DEFAULT = 0.0
RALT	= Receiver altitude in km - DEFAULT = 0.0
INCL	= Inclination of transmitting antenna with respect to the vertical in degrees - DEFAULT = 0.0.
THETA	= Orientation of transmitting antenna's projection in the horizontal plane with respect to the direction of propagation in degrees - DEFAULT = 0.0.

```

NAME
&DATUM
NPRINT=3,
DMAX=3., SIZE1=6.,
&END
DATA
FASTMC TEST, D=0
R 0.0 F 31.1350 A 208.234 C 4.388 M 5.6000-05 S 4.6400 00 E 81.0
1 89.78599 -6.258922-8.017555190-06-3.143704390-06-1.756763580-12-6.237969110-13
2 89.78599 -6.258922-3.668850850-09-1.806211180-09 9.486739700-01-1.861142440-01
1 88.98413 -1.682941 4.552990030-03-1.987877290-02-2.714797040-12 2.655112840-12
2 88.98413 -1.682941-2.440345930-07-1.551706140-07 9.594997620-01-1.699363550-01
1 83.31784 -0.608891 1.250675330-03-2.336613450-02-3.815659600-12 2.185022450-12
2 83.31784 -0.608891-2.606045880-07-1.909885790-07 9.715031320-01-1.463155000-01
1 78.98910 -0.665431 9.730016340-04-2.029831050-02-1.555728760-11-3.427403330-12
2 78.98910 -0.665431-3.220533350-07-4.715668900-07 9.901953500-01-1.042478400-01
1 74.97312 -0.764111 1.234872600-04-1.967820050-02-1.086145450-11-2.846834350-11
2 74.97312 -0.764111-1.191894540-07-7.552847030-07 1.010702380 00-3.736264340-02

R 1.000 F 31.1350 A 208.234 C 4.388 M 5.6000-05 S 1.0000-05 E 5.0
1 89.68035 -5.566901-1.241829790-05 1.278074990-04 7.365554290-09 2.507921680-08
2 89.68035 -5.566901 4.142102910-09-1.856645390-06 9.507347510-01-1.821507030-01
1 86.05721 -1.194791 4.486359910-04 1.682497450-03 7.855075460-08 2.618027010-07
2 86.05721 -1.194791-6.504312160-06-2.147211960-05 9.616847730-01-1.601697970-01
1 80.93273 -1.269851 2.843831290-03 5.426064250-03 2.449055440-07 5.717887800-07
2 80.93273 -1.269851-2.271621200-05-5.700980450-05 9.746484130-01-1.234766740-01
1 76.61480 -1.636121 1.082251110-02 1.109913520-02 1.935805520-08 8.073643290-07
2 76.61480 -1.636121-4.015206360-05-1.050856940-04 9.872011640-01-6.430890030-02
1 72.32836 -2.025471 3.268147330-02 6.000310250-03-5.460156510-07 7.302262140-07
2 72.32836 -2.025471-6.720166230-05-1.616247640-04 9.871700830-01 2.670312490-02

R 1.500 F 31.1350 A 208.234 C 4.388 M 5.6000-05 S 4.6400 00 E 81.0
1 89.78599 -6.258922-8.017555190-06-3.143704390-06-1.756763580-12-6.237969110-13
2 89.78599 -6.258922-3.668850850-09-1.806211180-09 9.486739700-01-1.861142440-01
1 88.98413 -1.682941 4.552990030-03-1.987877290-02-2.714797040-12 2.655112840-12
2 88.98413 -1.682941-2.440345930-07-1.551706140-07 9.594997620-01-1.699363550-01
1 83.31784 -0.608891 1.250675330-03-2.336613450-02-3.815659600-12 2.185022450-12
2 83.31784 -0.608891-2.606045880-07-1.909885790-07 9.715031320-01-1.463155000-01
1 78.98910 -0.665431 9.730016340-04-2.029831050-02-1.555728760-11-3.427403330-12
2 78.98910 -0.665431-3.220533350-07-4.715668900-07 9.901953500-01-1.042478400-01
1 74.97312 -0.764111 1.234872600-04-1.967820050-02-1.086145450-11-2.846834350-11
2 74.97312 -0.764111-1.191894540-07-7.552847030-07 1.010702380 00-3.736264340-02

R 40.
NAME
&DATUM NPRINT=1, TALT=6., RALT=6., INCL=90., THETA=90., &END
START
NAME
&DATUM INCL=0., THETA=0., NPLOT=1, NPRINT=0, ICOMP=2, &END
START
NAME
&DATUM INCL=90., THETA=90., &END
START

```

Figure 1. Sample card deck for FASTMC.

TOPHT = Height of the bottom of the ionosphere in km [integration limit h in equations (49) - (53)] - DEFAULT = 90.0

NPRINT = Flag to control printout of mode conversion and mode sum results
= 0 gives no printout
= 1 gives printout of mode parameters and calculated fields vs. distance - DEFAULT
= 2 also prints the input mode constants cards and the mode conversion coefficients
= 3 also prints the integrals used in the calculation of the mode conversion coefficients.

NAPLOT = Flag to control amplitude plots
= 0 gives no plot of amplitude
= 1 gives amplitude plots - DEFAULT

AMPMIN = Minimum amplitude to be plotted in dB above one microvolt/meter - DEFAULT = 10.0.

AMPMAX = Maximum amplitude to be plotted - DEFAULT = 70.0

AMPINC = Tic mark interval (for plot border) - DEFAULT = 10.0

NPLOT = Flag to control plots of phase relative to the speed of light
= 0 gives no plot - DEFAULT
= 1 gives phase plots

PHSMIN = Minimum phase excursion in degrees - DEFAULT = 360.0

PHSMAX = Maximum phase excursion - DEFAULT = 360.0

PHSINC = Tic mark interval (for plot border) - DEFAULT = 90.0

DMIN = Minimum distance from the transmitter in Mm - DEFAULT = 0.0
 DMAX = Maximum distance - DEFAULT = 10.0
 XINC = Horizontal tic mark intervals (for plot border) - DEFAULT = 1.0
 SIZEX = Length of horizontal axis in inches - DEFAULT = 10.0
 SIZEY = Length of vertical axis. Maximum value is 9.0 - DEFAULT = 6.0
 NRCURV = Number of sets of data to be plotted in one graph. Maximum value is 4 - DEFAULT = 1
 NRPTS = Number of data points to be calculated. Maximum value is 501 - DEFAULT = 501
 TOTAPE = Binary output flag
 = 0 gives no output - DEFAULT
 = 1 writes the complex mode sum and path parameters to logical unit 2
 TLONG,TLAT = Transmitter coordinates in degrees west and north - DEFAULT = 0.0, 0.0
 RBEAR = Path bearing in degrees clockwise from north - DEFAULT = 0.0

After reading the NAMELIST the program reads the next control card.

DATA Signals that the propagation path data follow. The format of this data is that which is produced by MODESRCH (Morfitt and Shellman, 1976), WAVEGUID (Pappert et al, 1970) and the INTEGRATED PREDICTION PROGRAM (Ferguson, 1972). The first

card contains the data set identification. This card is used to supply a literal path description such as "HAWAII TO WAKE". This is followed by sets of mode constants, one for each path segment or slab. The first card for each segment contains the starting distance (ρ), frequency (f), magnetic azimuth, codip and intensity, ground conductivity and permittivity (σ , ϵ), and the nominal height of the free space portion of the waveguide (h). Of these parameters, ρ , f , σ , and ϵ must appear. The magnetic parameters are included for reference. The value of h may be included if it is to vary among the segments. Otherwise it is a constant value input via the NAMELIST. This card is followed by the mode constants cards, one pair for each mode, containing the following information:

1	θ	I	T_1	T_2
2	θ	I	T_3	T_4

where 1 and 2 are sequencing indices, θ is the complex eigenangle at the ground, I is an index indicating the functional form of the ratio e_y/h_y [equation (28)] and the T s are complex constants described below.

The list of modes for each segment is terminated by a blank card. A maximum of 20 modes will be used although there is no maximum number which the data deck may contain. The list of segments is terminated by a card with $\rho = 40$. Parameters for each segment are stored sequentially on logical file 4. The number of path segments is limited by the space allocated to this file. Each segment requires 1848 words of storage. After reading these data the program generates the required calculations (as specified by the NAMELIST input or defaults) then returns for another control card.

BUMP Signals that this card contains an overall plot identification. It is used for additional information not contained in the data set identification cards. When several sets of data are plotted on one graph, it can be used to provide a connection between them.

START Signals calculations using new NAMELIST parameter values for the current propagation path data.

A summary of how the control cards are used in FASTMC is shown in figure 2. A brief description of the subroutine functions is given in table 1, and complete listings can be found in appendix A. Sample plotted outputs are shown in figures 3 and 4. The T_s on the data cards are given by the following relationships:

$$T_1 = \frac{(1 + \bar{R}_1)^2 (1 - \bar{R}_1 \bar{R}_1) s^{1/2}}{\frac{\partial F}{\partial \theta} \bar{R}_1 f_1^2(d)}$$

$$T_2 = \frac{(1 + \bar{R}_1)^2 (1 - \bar{R}_1 \bar{R}_1) s^{1/2}}{\frac{\partial F}{\partial \theta} \bar{R}_1 f_1^2(d)}$$

$$T_3 = \frac{(1 + \bar{R}_1)(1 + \bar{R}_1 \bar{R}_1) s^{1/2}}{\frac{\partial F}{\partial \theta} f_1(d) f_1(d)}$$

$$T_4 = \frac{\bar{R}_1}{\bar{R}_1} .$$

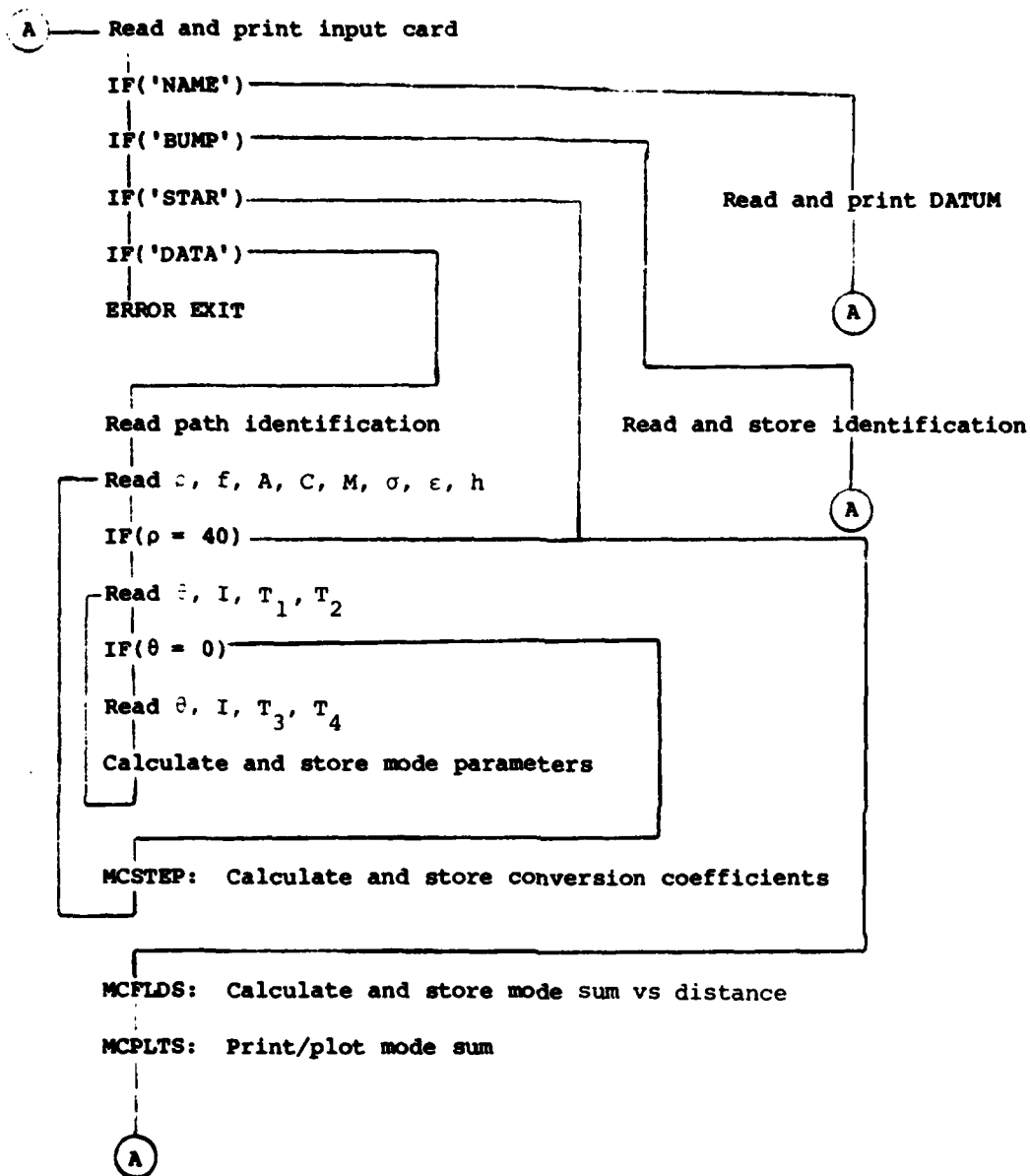
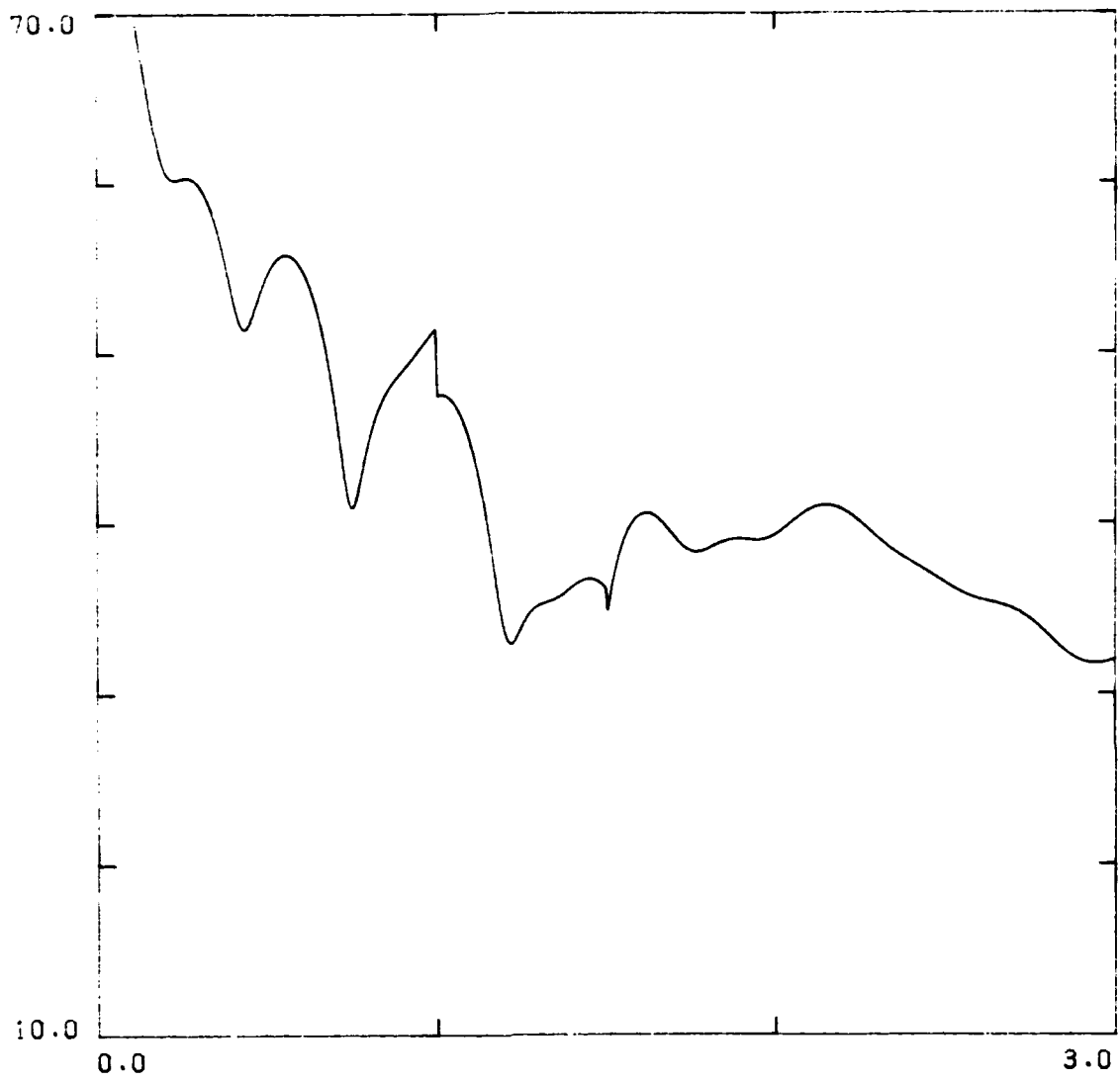


Figure 2. Illustration of FASTMC program execution sequence.

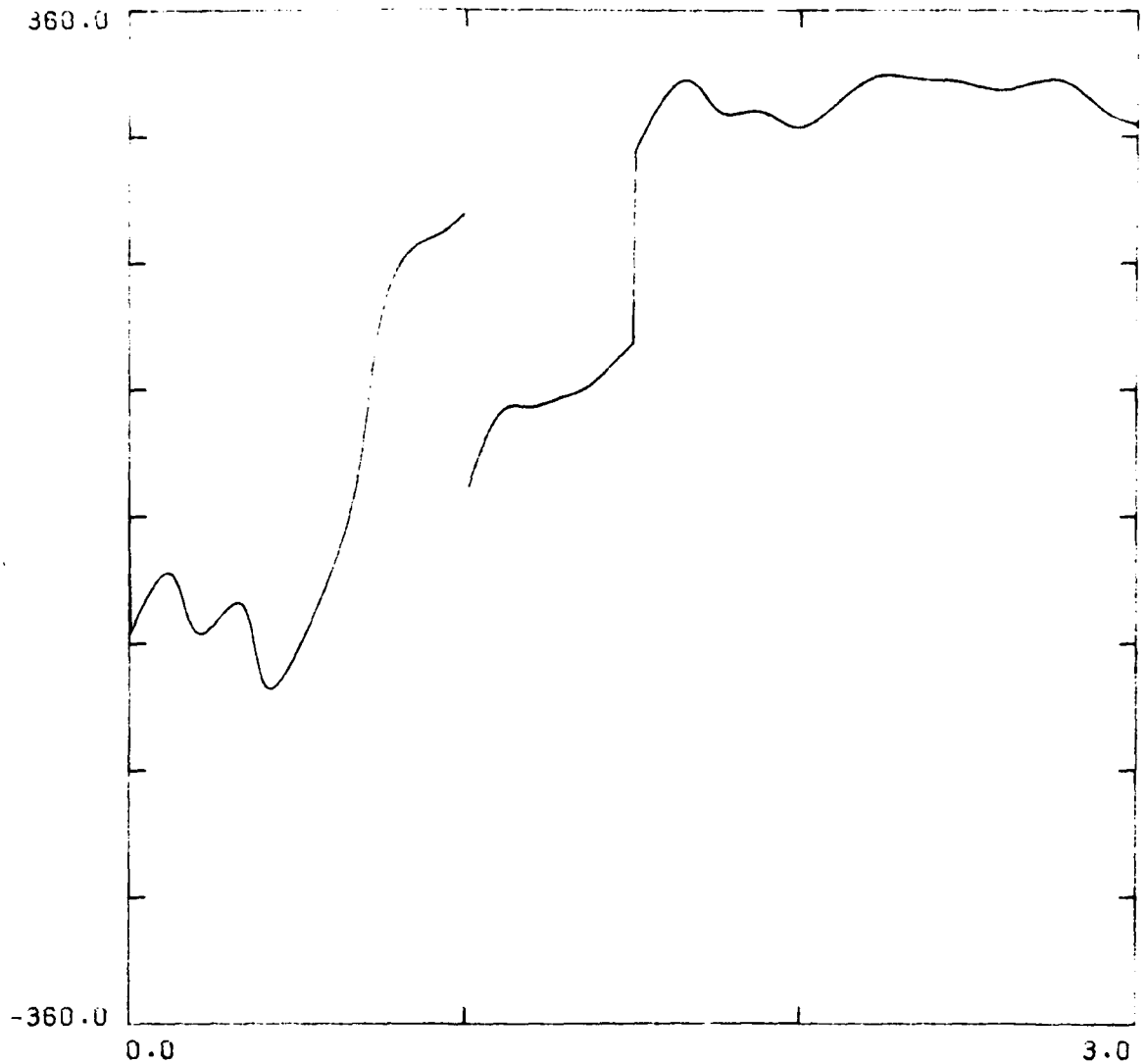
MCSTEP	Calculates the integrals (50) and solves for the conversion coefficients (44) at each segment boundary. Calls MDHNKL and CLINEQ.
MCFLDS	Calculates the field strength from DMIN to DMAX. Calls HTGAIN.
MCPLTS	Prints and plots amplitude and phase. Calls BORDER, CURVE, and CALCOMP routines.
MDHNKL	Calculates modified Hankel functions of order one-third and their derivatives.
HTGAIN	Calculates height-gain functions (32, 33). Calls MDHNKL.
CLINEQ	Solves system of equations for complex coefficients.
BORDER	Draws border for plots. Labels minimum and maximum values of axes.
CURVE	Draws a curve of x vs y. Seven different line types are available. FASTMC uses only the first four types: solid, long, medium, and short dashes.

Table 1. FASTMC subroutines.



0.0
 FMC 1
 Z COMPONENT AMPLITUDE POWER = 1. FREQ = 31.135
 INCL = 0. THETA = 0. TALT = 0.0 RALT = 0.0
 FASTMC TEST, D=0

Figure 3. Sample plot of amplitude output from FASTMC. This is the first plot generated by the card deck of figure 1.



0.0 3.0
 FMC 4
 Y COMPONENT RELATIVE PHASE FREQ = 31.135
 INCL = 0. THETA = 0. TALT = 6.0 RALT = 6.0
 FASTMC TEST, D=0

Figure 4. Sample plot of relative phase output from FASTMC. This is the fourth plot generated by the card deck of figure 1.

From these relationships, equation (26) can be written as follows:

$$H_Y = - \frac{k_o^{-5/2} e^{-i\pi/4} S}{2\epsilon_o \sqrt{2\pi} a \sin(D/a)} T_1 f_I(z_T) f_I(z_R) e^{-ik_o S}, \quad (61)$$

and equation (28) can be evaluated at the ground, giving the relationship

$$\gamma = \frac{e_y}{h_y} = \frac{(1 + \bar{R}_I) \bar{R}_I R_I}{(1 - \bar{R}_I R_I)(1 + \bar{R}_I)} \frac{f_I(d)}{f_I(d)} = \frac{T_3}{T_1}, \quad (62)$$

where f_I , f_I are from equations (53) and (54).

The relationship in equation (62) is used if the value of I on the mode cards is 1. If the value of I is 2, the following relationship is used:

$$\gamma = \frac{(1 + \bar{R}_I)(1 - \bar{R}_I R_I)}{(1 + \bar{R}_I) \bar{R}_I R_I} \frac{f_I(d)}{f_I(d)} = \frac{T_2}{T_3 T_4}. \quad (63)$$

Equations (62) and (63) are identical if the value of the mode equation (12) is exactly zero. The value of I is determined from the mode polarization as calculated in the WAVEGUID, MODESRCH, or INTEGRATED PREDICTION PROGRAM. A mode which is principally TM will have $1 - \bar{R}_I \bar{R}_I$ very small and the ratio γ will be very large, resulting in the use of equation (62). Conversely, a mode

which is principally TE will have $1 - \frac{R_1}{\bar{R}_1}$ very small, and the ratio γ will be very small, resulting in the use of equation (63).

The excitation factor for H_y due to a vertical radiator can be defined from equation (61) as $-ST_1$. Excitation factors due to horizontal end-fire and horizontal broadside radiators can be obtained from Pappert et al, 1970. In terms of the T_s , these are T_1 and T_3T_4 for end-fire and broadside, respectively. The corresponding electric field components are obtained from equation (55).

5. BUMP

BUMP is a computer program which has been written to allow for a systematic variation of a path perturbation, with full allowance for variation of the mode parameters with conductivity and magnetic field. The most common perturbation is the day-night terminator. Previous studies of the effect of the terminator on propagation were limited to waveguides for which the magnetic field and ground conductivity were constant. BUMP allows for the study of the effect of the terminator along a path with mixed ground conductivities and/or significant magnetic field variations along the propagation path. The formulation of the program allows for other perturbations to be studied.

The design of the program was aimed at requiring the simplest possible data deck preparation. This was done in order to make it easy to modify propagation path data and to allow flexibility in the ionospheric models. The resulting input requires propagation path data for a series of horizontally homogeneous ionospheres. The data for each ionosphere are merged by the program to produce the required ionospheric perturbation. This program has been used to study models of the ionospheric variation from middle to high latitudes and to study trans-terminator propagation across the magnetic equator. The program to be described below is set up for a minimum path segment length of 5 km and a maximum path length of 40 Mm. This requires 801 random access records per ionosphere. Since a substantial portion of the cost of running the program is incurred in setting up the random access files required, users can achieve some cost savings by changing the 5 km and 40 Mm figures and modifying the random access files accordingly. A maximum of 30 modes can be stored for each path segment, requiring 1229 words of storage in each random access record.

Preparation of the input data for this program is illustrated for a bump in the ionosphere. The lowest height of ionosphere will be characterized by $h' = h_0$ and the highest height by $h' = h_6$. The variation of the ionosphere from lowest to highest is modeled by a linear variation of h' over six steps denoted by h_1, h_2, h_3, h_4, h_5 . The length of each step is $\Delta\rho_1$ and the length of the step at h_6 is $\Delta\rho_2$. The bump in the propagation path is defined in figure 5.

By making $\Delta\rho_2$ equal to 20 Mm, the bump becomes a ramp for modeling the day-night transition. If the order of input of the data sets corresponding to each h' were reversed, the ramp would model the night-day transition. Movement of the bump is accomplished by varying ρ from ρ_0 to ρ_L in increments of $\Delta\rho$. If ρ_0 is greater in value than ρ_L , the sign of $\Delta\rho$ is adjusted automatically. The total path length is ρ_{max} .

If the data set for h_n does not have data corresponding to $\rho + (n - 1)\Delta\rho_1$, the data from the next smaller distance is used. For example, suppose h_n has data at 1.0 Mm and 1.2 Mm and $\rho + (n - 1)\Delta\rho_1$ is greater than 1.0 Mm and less than 1.2 Mm. The program will select the data for 1.0 Mm to be used at $\rho + (n - 1)\Delta\rho_1$. If the value of ρ becomes less than zero, the necessary steps in h_n are removed. For example, if $\rho = -1.5\Delta\rho_1$, the first step on the propagation path will be h_2 . A similar procedure is followed if $\rho + (n - 1)\Delta\rho_1$ becomes greater than ρ_{max} .

The input to BUMP is a series of FASTMC compatible data sets, one for each ionospheric profile. Each data set must contain data for the required propagation path. The output from BUMP is a series of FASTMC data sets, each corresponding to one position of the bump or ramp on the propagation path. The data set identification card which follows each "DATA" card contains the values of ρ , $\Delta\rho_1$, $\Delta\rho_2$, and the h_s heights. An additional identification card corresponding to the FASTMC input control card "BUMP" may be output.

The order of execution of the program is specified by a set of control cards. Each card is read and printed in its entirety, but only the first four columns are examined by the program. These control cards and their functions are described below.

NAME signals that NAMELIST data follows. The NAMELIST is DATUM. The input variables are defined as follows:

RHO0 = ρ_0 in Mm - DEFAULT = 1.0

RHOL = ρ_L in Mm - DEFAULT = 2.0

DRHO = $\Delta\rho$ in Mm - DEFAULT = 0.1

DRHO1 = $\Delta\rho_1$ in Mm - DEFAULT = 0.1

DRHO2 = $\Delta\rho_2$ in Mm - DEFAULT = 20.0

RHOMAX = ρ_{\max} in Mm - DEFAULT = 10.0

HPRIME = h' in km. Maximum number of values is 7 - DEFAULT =
87.0, 85.0, 83.0, 81.0, 79.0, 77.0, 75.0

ID signals that the next card is to be read for identification of the output. The first 76 columns of this card are stored on a card with BUMP in its first 4 columns. This can be processed by FASTMC.

DATA signals that data corresponding to one of the values of h' follow. These data are in the same format as required by FASTMC. They must be input in the order indicated by the HPRIMEs in the NAMELIST. The data for HPRIME(n) are stored in logical file 10 + n. The individual segments are stored in random access files, with each record representing a multiple of 5 km with a maximum distance of 40 Mm. Thus, data at 1.234 Mm will be stored as 1.235 Mm in record number 248.

START signals that all necessary inputs are complete and the generation of the output data sets is to begin. The output is written to external file "OUTPUT" (logical file 2) in FASTMC card image format.

The resulting data are used in FASTMC to obtain the variation of field strength parametric in the position of the perturbation. Various programs exist or could be written to display this output in other forms. Appendix B is a listing of the program.

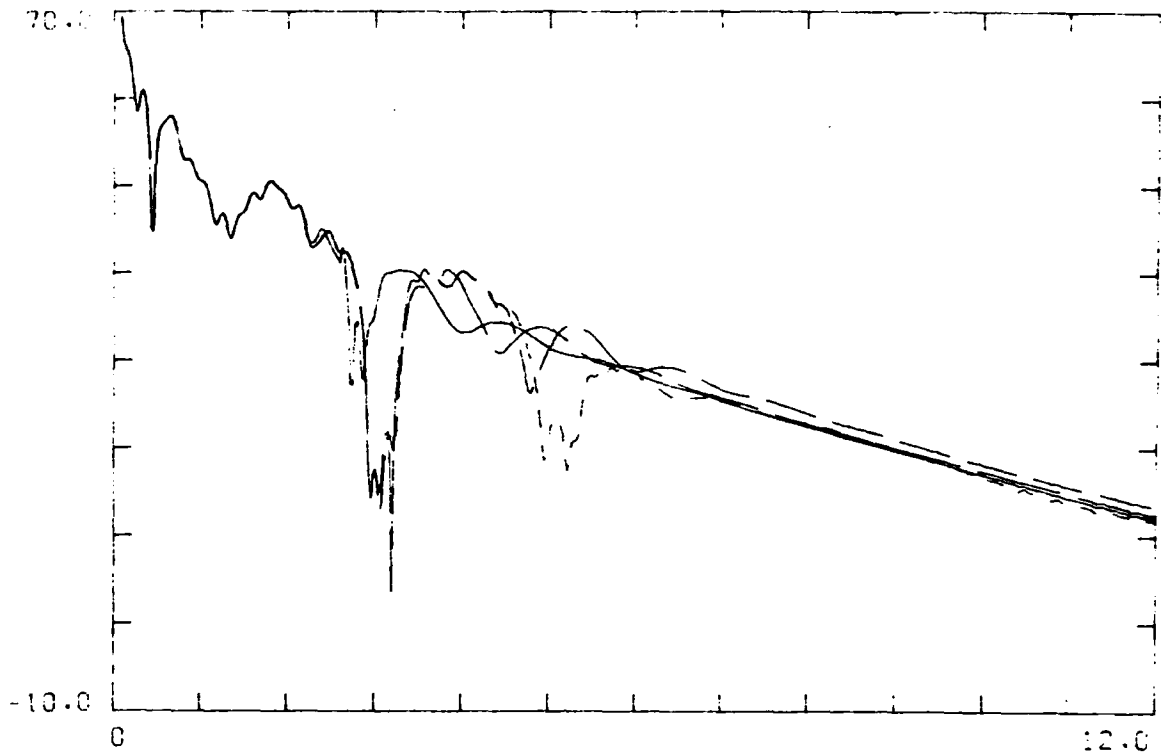
To illustrate the execution of BUMP with FASTMC, let us assume that a file named NLK exists. This file contains data elements for a variety of ionospheric profiles on the propagation path NLK to Brisbane, Australia. The electron density profile is exponential in height with a slope β and a reference height h' denoted by β/h' . The data elements in NLK are renamed BBHH, where BB and HH denote β and h' , respectively. For example, the daytime ionosphere is taken to be 0.3/74 and the corresponding data element is named 3074. The nighttime ionosphere is taken to be 0.5/86. The variation in ionosphere from day to night is made in five equally spaced steps in β and h' . The output from BUMP is to go into a temporary file named OUTPUT, which is to be used in FASTMC to generate the resulting mode sums. The data deck to carry out these operations is shown in figure 6. The resulting plot is shown in figure 7. Note that the use of the "ID" control card in the input to the BUMP program results in additional identification of the curves via the "BUMP" control card in FASTMC. Also note that although β as well as h' varies, there is provision for identifying only the latter; the β variation must be indicated in the "ID" card.

```

@ASS.T OUTPUT.,F///1000
@XQT PGM.BUMP
ID
NLK TO BRISBANE, NIGHT (0.5/86) TO DAY (0.3/74)
NAME
  &DATUM RH00=2., RH01=5., DRHO=1., DRHO1=.150,
  RHOMAX=12.,
  HPRIME=86., 84., 82., 80., 78., 76., 74.,
  &END
@ADD NLK.5086
@ADD NLK.4784
@ADD NLK.4382
@ADD NLK.4080
@ADD NLK.3778
@ADD NLK.3376
@ADD NLK.3074
START
@XQT PGM.FASTMC
NAME
  &DATUM NPRINT=0, NRCURV=4, DMAX=12., SIZEX=6., AMPMIN=-10., SIZEY=4., &END
@ADD OUTPUT.

```

Figure 6. Sample card deck for running BUMP and FASTMC.



```

FMC 1
Z COMPONENT AMPLITUDE POWER = 1.   FREQ = 19.500
INCL = 0.   THETA = 0.   TALT = 0.0   RALT = 0.0
BUMP NLK TO BRISBANE, NIGHT (0.5/95) TO DAY (0.3/74)
----- RHC= 2.00 DRHC1= .15 DRHC2=20.00 d1= 96. 84. 92. 80. 73. 75. 74.
----- RHC= 3.00 DRHC1= .15 DRHC2=20.00 d1= 96. 84. 92. 80. 73. 75. 74.
----- RHC= 4.00 DRHC1= .15 DRHC2=20.00 d1= 96. 84. 92. 80. 73. 75. 74.
----- RHC= 5.00 DRHC1= .15 DRHC2=20.00 d1= 96. 84. 92. 80. 73. 75. 74.

```

Figure 7. Plots from data deck of figure 6.

REFERENCES

- Abbas, MM, Pidwell, DW and Walsh, EJ (1971), Propagation of VLF waves below generally anisotropic ionospheres, Can. Jour. Phys., v. 49, 1040.
- Araki, T. (1973), Anomalous diurnal changes of transequatorial VLF radio waves, J. Atmos. Terr. Phys., v. 35, 693.
- Araki, T., Kitayama, S. and Susumu, K. (1969), Transequatorial reception of VLF radio waves from Australia, Radio Science, v. 4, no. 4, 367.
- Bickel, JE, Ferguson, JA and Stanley, GV (1970), Experimental observation of magnetic field effects on VLF propagation at night, Radio Sci., v. 5, no. 1, 19.
- Budden, KG (1961a), The waveguide mode theory of wave propagation, Logos Press, London.
- Budden, KG (1961b), Radio waves in the ionosphere, Cambridge University Press, Cambridge.
- Budden, KG (1962), The influence of the earth's magnetic field on radio propagation by wave-guide modes, Proc. Roy. Soc. London, A, 265, 538.
- Budden, KG and Martin, HG (1962), The ionosphere as a whispering gallery, Proc. Roy. Soc. London, A265, 554-569.
- Chilton, CJ, Crary, JH (1971), VLF observations of nighttime D-region ionization enhancement by the Scorpius XR-1 X-ray source, Radio Sci. v. 6, no. 7, 699.
- Chilton, CJ, Diede, AH and Radicella, SM (1964), Transequatorial reception of very-low-frequency transmission, J.G.R., v. 69, no. 7, 1319.
- Computation Laboratory Staff at Cambridge, Mass. (1945), Tables of the modified Hankel function of order one-third and of their derivatives, Harvard University Press, Cambridge, Mass.
- Crombie, DD (1964), Periodic fading of VLF signals received over long paths during sunrise and sunset, Radio Sci. J. Res. NBS, 68D, no. 1, 27.
- Deeks, DG (1966), D-region electron distributions in middle latitudes, Proc. Roy. Soc. London, A291, 413.
- Ferguson, JA (1968), Effects of earth's magnetic field on VLF waveguide modes, NOSC Technical Note NELC TN 1398. NOSC TNs are informal documents intended chiefly for internal use.
- Ferguson, JA (1972), An Improved Integrated Prediction Program, NOSC Technical Note NELC TN 2231, 11 December.

Foley, G, Wand, IC, and Jones, TB (1973), Studies of the modal parameters of VLF radiowaves propagated below the night-time ionosphere, J. Atmos. Terr. Phys., v. 35, 2111.

Friedman, B. (1959), Principle and Techniques of Applied Mathematics, Wiley, New York.

Galejs, J. (1971), VLF propagation across discontinuous daytime to nighttime transitions in anisotropic terrestrial waveguide, IEEE Trans. Ant. Prop., AP-19(6), 756.

Galejs, J. (1972), Terrestrial propagation of long electromagnetic waves, Pergamon Press, Oxford.

Kaiser, AB (1968), Latitude variation in VLF modal interference, Radio Sci., v. 3 (new series), no. 11, 1084.

Lynn, KJW (1967), Anomalous sunrise effects observed on a long transequatorial VLF propagation path, Radio Sci., v. 2 (new series), no. 6, 521.

Lynn, KJW (1969), Multisite observations of the VLF transequatorial propagation anomaly, Radio Sci., v. 4, no. 3, 203.

Lynn, KJW (1970), The interpretation of transequatorial VLF sunrise observations, J. Atmos. Terr. Phys., v. 32, 57.

Lynn, KJW (1978), Some differences in diurnal phase and amplitude variations for VLF signals, J. Atmos. Terr. Phys., v. 40, 145.

Makarov, GI, Novikov, VV and Orlov, AB (1970), Modern state of investigations of the propagation of ultralong waves in the earth-ionosphere waveguide channel (review), Izv. Radiofizika, v. 13, no. 3, 321.

Meara, LA (1973), VLF modal interference effects observed on transequatorial paths, J. Atmos. Terr. Phys., v. 35, 305.

Morfitt, DG and Shellman, CH (1976), "MODESRCH", An Improved Computer Program for Obtaining ELF/VLF/LF Mode Constants in an Earth-Ionosphere Waveguide, Defense Nuclear Agency Interim Report 77T, 1 October.

Morse, PM and Feshbach, H (1953), Methods of Theoretical Physics, McGraw-Hill, New York.

Pappert, RA (1968), A numerical study of VLF mode structure and polarization below an anisotropic ionosphere, Radio Sci., v. 3, no. 3, 219.

Pappert, RA, Moler, WF and Shockey, LR (1970), A FORTRAN program for waveguide propagation which allows for both vertical and horizontal dipole excitation, Defense Atomic Support Agency Interim Report 702.

Pappert, RA and Shockey, LR (1974), A simplified mode conversion program for VLF propagation in the earth-ionosphere waveguide, Defense Nuc. Agency Interim Report 751.

- Pappert, RA and Smith, RR (1972), Orthogonality of height-gains in the earth-ionosphere waveguide, *Radio Science*, v. 7, 275.
- Pappert, RA and Snyder, FP (1972), Some results of a mode-conversion program for VLF, *Radio Sci.*, v. 7, no. 10, 913.
- Richter, JH (1966), Applications of conformal mapping to earth-flattening procedures, *Radio Sci.*, v. 1 (new series), no. 12, 1435.
- Round, HJ, Eckersley, JL, Tremellen, K. and Lunnon, FC (1925), Report on measurements made on signal strength at great distances during 1922 and 1923, *I.E.E.E.*, 63, 933.
- Schumann, WO, (1952), On the radiation free self oscillations of a conducting sphere, which is surrounded by an air layer and an ionospheric shell (in German), *Z. Naturforsch.*, 72, 149.
- Schumann, WO (1954), Uber die Strahlung langer Wellen des horizontalen Dipols in dem Lufthohlraum zwischen Erde und Ionosphare I, *Zeitschrift fur angewandte Physik*, 6, 225.
- Smith, RA, Coyne, TN, Lock, RG and Bourne, IA (1968), Ground based radio wave propagation studies of the lower ionosphere, *D.R.T.E.*, Ottawa, Canada, 335.
- Smith, RA (1974), Approximate mode conversion coefficients in the earth-ionosphere waveguide for VLF propagation below an anisotropic ionosphere, *J. Atmos. Terr. Phys.*, v. 36, 1683.
- Snyder, FP (1968a), Mode numbering for an exponential anisotropic ionosphere, *NOSC Technical Note NELC TN 1394*.
- Snyder, FP (1968b), Effect of magnetic dip-angle and azimuth-angle variations on mode numbering at VLF, *NOSC Technical Note NELC TR 1587*.
- Snyder, FP and Pappert, RA (1969), A Parametric Study of VLF Modes Below Anisotropic Ionospheres, *Radio Science*, 4, 213.
- Sommerfeld, A. (1949), *Partial differential equations in physics*, Academic Press, New York.
- Svennesson, J. and Westerlund, S. (1979), Stellar X-ray effects on VLF radiowave propagation, *J. Atmos. Terr. Phys.*, v. 41, 361.
- Wait, JR (1961), A new approach to the mode theory of VLF propagation, *J. Res. NBS*, 65D (Radio Prop.), no. 1, 37.
- Wait, JR (1962), *Electromagnetic waves in stratified media*, Macmillan, New York.
- Wait, JR (1964), Two-dimensional treatment of mode theory of the propagation of VLF radio waves, *Radio Sci.*, v. 68D, no. 1, 81.
- Wait, JR (1968a), Mode conversion and refraction effects in the earth-ionosphere waveguide for VLF radio waves, *J. Geophys. Res.*, 73(11), 3537.

Wait, JR (1968b), On the theory of VLF propagation for a step model of the nonuniform earth-ionosphere waveguide, *Can. J. Phys.*, 46(17), 1979.

Wait, JR and Spies, KP (1963), Height gain for VLF radiowaves, *J. Res. NBS (Radio Prop)*, 67D, 183-187.

Wait, JR and Spies, KP (1964), Characteristics of the earth-ionosphere waveguide for VLF radiowaves, *NBS Tech. Note* 300.

Walker, D. (1965), Phase steps and amplitude fading of VLF signals at dawn and dusk, *Radio Sci.*, (J. Res. NBS), 69D, 1435.

Watson, GN (1918), The diffraction of radio waves by the earth, *Proc. Roy. Soc. London*, A95, 83-99.

Watson, GN (1919), The transmission of electric waves around the earth, *Proc. Roy. Soc.*, A95, 546-563.

Watson, GN (1944), *The theory of Bessel Functions*, Cambridge University Press, Cambridge.

APPENDIX A:

FASTMC

```

1
2
3
4
5
6
7
8
9
10
11
12
13
14
15
16
17
18
19
20
21
22
23
24
25
26
27
28
29
30
31
32
33
34
35
36
37
38
39
40
41
42
43
44
45
46
47
48
49
50
51
52
53
54
55
56

C APPROXIMATE MODE CONVERSION
C
C IMPLICIT REAL*8 (A-H,O-Z)
COMMON/MC INPI/XTRA(3,20),TERM(20),FREQ,OMEGA,WAVENO,MIK,
$ ALPHA,AK,KA13,KA23,NGSQ,NTHSQ,CONST,ACONST,ECONST
COMMON/MC STOR/A(20,20),FOFR(20),S(20),TP(20),XVAL,SIGMA,EPSR,
$ NRMODE,NRSLAB
COMMON/MC PLOT/DMIN,DMAX,XINC,AMPMIN,AMPMAX,AMPINC,PHSMIN,PHSMAX,
$ PHSINC,DPLOT(20),BUMPID(20),FRQ,POWER,ICOMP,INCL,THETA,
$ TALT,RALT,IDENT,NRPTS,SIZE1,SIZE2,DATE,TIME,NRCURV,
$ NRCRVS,NRPLTS,NAPLOT,NPLOT,NPRINT
COMMON SUMOUT(501)
COMPLEX*16 TP,A,S,FOFR,XTRA,TERM,NGSQ,MI/(0.00,-1.00),MIK,
$ TRP1,TMP2,TMP3,TMP4,RATIO(4)
COMPLEX*8 SUMOUT
REAL*8 KA13,KA23,NTHSQ
REAL*4 DMIN,DMAX,XINC,AMPMIN,AMPMAX,AMPINC,PHSMIN,PHSMAX,PHSINC,
$ SIZE1,SIZE2,SIZEY1,FRQ,TPHT,TALT,RALT,
$ INCL,THETA,TLONG,TLAT,RBEAR,POWER
INTEGER TOTAPE
CHARACTER*8 DATE,TIME
CHARACTER*4 BCD,PLOTID,BUMPID
CHARACTER LABEL,IDENT
C ICOMP RECEIVED COEFFICIENT, =1 IS Z, =2 IS Y
C INCL,THETA ORIENTATION OF TRANSMITTER ANTENNA
C TALT,RALT TRANSMITTER, RECEIVER ALTITUDE IN KM
C TOPHT HEIGHT OF THE BOTTOM OF THE IONOSPHERE IN KM
C DMIN,DMAX,XINC DISTANCE RANGE AND TIC INTERVAL IN MM
C NAPLOT AMPLITUDE PLOT FLAG
C AMPMIN,AMPMAX,AMPINC AMPLITUDE PLOT RANGE AND TIC INTERVAL IN DB
C NPLOT PHASE PLOT FLAG
C PHSMIN,PHSMAX,PHSINC PHASE PLOT RANGE AND TIC INTERVAL IN DEGREES
C SIZE1,SIZE2 AXIS LENGTHS IN INCHES
C SIZEY1,SIZEY2 AXIS LENGTHS IN INCHES
C NRCURV NUMBER OF CURVES PER GRAPH, MAX OF 4
C NRPTS NUMBER OF POINTS TO OUTPUT, MAX OF 501
C NPRINT PRINTOUT FLAG
C TOTAPE OUTPUT FLAG, =1 WRITES IO LOGICAL UNIT 2
C TLONG,TLAT TRANSMITTER LOCATION IN DEGREES WEST,NORTH
C RBEAR PATH BEARING IN DEGREES EAST OF NORTH
C POWER RADIATED POWER IN KW
C
C NOTE: TLONG,TLAT,RBEAR ARE FOR TOTAPE=1 OUTPUT ONLY
C
C NAMELIST/DATUM/ICOMP,INCL,THETA,TALT,RALT,TPHT,
$ NAPLOT,NPLOT,NPRINT,NRCURV,SIZE1,SIZE2,
$ SIZEY1,SIZEY2,AMPMAX,AMPMIN,AMPINC,PHSMAX,PHSMIN,PHSINC,
$ DMAX,DMIN,XINC,TLONG,TLAT,RBEAR,POWER,TOTAPE,NRPTS
C
C DIMENSION STORE(924),BCD(20),LABEL(2)
C EQUIVALENCE (STORE,A),(SIZE1,SIZEY1),(SIZE2,SIZEY2)
C DATA LABEL,'Z','Y',/
C DATA EPSLN0/B.854340-12/,ALPHA/3.140-04/,DTR/.0174532925200/
C DATA ICOMP/1/,INCL,THETA/0.0./,TALT,RALT/0.0./,TOPHT/90.00/

```

```

57 DATA TLONG,TLAT,RBEAR/0.,0.,0.,/ ,POWER/1./
58 DATA DMIN,DMAX,XINC/0.,10.,1./
59 DATA AMPMIN,AMPMAX,PHSINC/10.,70.,10./
60 DATA PHSMIN,PHSMAX,PHSINC/-360.,360.,90./
61 DATA SIZEZ,SIZEY/10.,6./
62 DATA NRPTS/501/,NRCURV/1/,NAPLOT/1/,NPLOT/0/,NPRINT/1/
63 DATA NRCRVS,NRPLTS/0/,BUMPID/20*,'/'
64
65 C GET DATE AND TIME FOR PLOT IDENTIFICATION
66 CALL ADATE(,DATE,TIME)
67 PRINT 1004,DATE,TIME
68
69 C GET CONTROL CARD
70 PRINT 1001
71 READ(5,1002,END=998) BCD
72 PRINT 1003,BCD
73 IF(BCD(1)) .EQ. 'NAME') GO TO 12
74 IF(BCD(1)) .EQ. 'BUMP') GO TO 15
75 IF(BCD(1)) .EQ. 'DATA') GO TO 20
76 IF(BCD(1)) .EQ. 'STAR') GO TO 30
77 GO TO 910
78
79 C READ NAMELIST
80 READ DATUM
81 PRINT DATUM
82 IF(NRCURV .GT. 4) GO TO 913
83 IF(SIZEY .GT. 9.) GO TO 918
84 IF(NRPTS .GT. 501) GO TO 919
85 GO TO 10
86
87 C STORE BUMP ID CARD
88 DO 16 I=1,20
89 BUMPID(I)=BCD(I)
90 GO TO 10
91
92 C READ PROPAGATION PATH DATA
93 READ(5,1002,END=915) IDPLOTT
94 PRINT 1003, IDPLOTT
95 NRMODE=20
96 NRSLAB=0
97 RHO=-1.
98 NTMSQ=1.+ALPHA*TOPHT
99 REWIND 4
100 READ(5,1020,END=915) RR,FF,AA,CC,BB,SS,EE,TH
101 IF(RR .NE. 40. .AND. SS .EQ. 0.) GO TO 21
102 XVAL=RR*1000.
103 IF(NRSLAB .GT. 0) WRITE(4) STORE
104 IF(RR .EQ. 40.) GO TO 25
105 NRSLAB=NRSLAB+1
106 NM=0
107 BB=BB*10000.
108 PRINT 1022,NRSLAB,RR,FF,AA,CC,BB,SS,EE,TH
109 IF(NPRINT .GE. 3) PRINT 1024
110 IF(RR .GT. 0.) GO TO 22
111 FROM=FF
112 FREQ=FF
113 CONST=682.2408*DSQRT(FREQ*POWER)

```

```

114 OMEGA=G.283185308D3*FREQ
115 WAVENO=20.958445D-3*FREQ
116 MIK=DCMPLX(0.D0,-WAVENO)
117 ACONST=-8.686D3*WAVENO
118 ECONST=20.*DLOG10(35.*WAVENO)
119 AK=ALPHA/WAVENO
120 AK13=DEXP(DLOG(AK)/3.D0)
121 KA13=1.D0/AK13
122 KA23=KA13**2
123 IF(RHO .GT. RR) GO TO 912
124 RHO=RR
125 SIGMA=SS
126 EPSR=EE
127 NGSQ=DCMPLX(EPSR,-SIGMA/(OMEGA.EPSLNO))
128 IF(TH .EQ. 0.) GO TO 23
129 NTHSQ=1.+ALPHA*TH
130 READ(5,1023,END=915) INDX1,TR1,TI1,ITRM1,TMP1,TMP2
131 IF(TR1 .EQ. 0.) GO TO 24
132 READ(5,1023,END=915) INDX2,TR2,TI2,ITRM2,TMP3,TMP4
133 IF(NM .EQ. 20) GO TO 233
134 IF(CDABS(TMP1) .EQ. 0.) GO TO 233
135 IF(TR1 .NE. TR2 .OR. TI1 .NE. TI2) GO TO 234
136 IF(ITRM1 .NE. ITRM2) GO TO 234
137 IF(ITRM1 .EQ. 0) GO TO 911
138 NM=NM+1
139 IF(NPRINT .LT. 3) GO TO 230
140 PRINT 1025,NM,INDX1,TR1,TI1,ITRM1,TMP1,TMP2,
141     INDX2,TR2,TI2,ITRM2,TMP3,TMP4
142 $
143 TP(NM)=DCMPLX(TR1,TI1)
144 S(NM)=CDSIN(TP(NM)*DTR)
145 RATIO(2,INDX1-1)=TMP1
146 RATIO(2,INDX2-1)=TMP3
147 RATIO(2,INDX2 )=TMP4
148 TERM(NM)=RATIO(4)
149 GET EY/HY
150 IF(ITRM1 .EQ. 2) GO TO 231
151 FOFR(NM)=RATIO(3)/RATIO(1)
152 GO TO 232
153 FOFR(NM)=RATIO(2)/(RATIO(3)*RATIO(4))
154 232 IF(NRSLAB .GT. 1) GO TO 23
155 C
156 C GET HY EXCITATION FACTOR AT THE TRANSMITTER
157 XTRA(1,NM)=-RATIO(1)*S(NM)
158 XTRA(2,NM)= RATIO(3)*RATIO(4)
159 XTRA(3,NM)= RATIO(1)
160 GO TO 23
161 IF(NPRINT .LT. 3) GO TO 23
162 PRINT 1026,     INDX1,TR1,TI1,ITRM1,TMP1,TMP2,
163     INDX2,TR2,TI2,ITRM2,TMP3,TMP4
164 $
165 IF(TR1 .NE. TR2 .OR. TI1 .NE. TI2) GO TO 916
166 IF(ITRM1 .NE. ITRM2) GO TO 917
167 GO TO 23
168 IF(NPRINT .LT. 3) PRINT 1027,NM
169 NRMODE=NM
170 C
171 C GET CONVERSION COEFFICIENTS

```

```

171 CALL MCSTEP
172 GO TO 21
173 IF(NRSLAB .LE. 1) GO TO 914
174 C
175 CALCULATE MODE SUM
176 IDENT=LABEL(ICOMP)
177 CALL MCFDLS
178 C
179 IF(TOTAPE .EQ. 0) GO TO 40
180 C
181 SAVE MODE SUM
182 WRITE(2) SUMOUT,FRQ,TLONG,TLAT,RBEAR,POWER,INCL,THETA,TALT,RALT,
183 $
184 C
185 MODE SUM OUTPUT
186 CALL MCPLTS
187 PRINT 1000
188 GO TO 10
189 C
190 ERROR EXITS
191 C
192 PRINT 1910
193 GO TO 998
194 PRINT 1911
195 GO TO 998
196 PRINT 1912
197 GO TO 998
198 PRINT 1913
199 GO TO 998
200 PRINT 1914
201 GO TO 998
202 PRINT 1915
203 GO TO 998
204 PRINT 1916
205 GO TO 998
206 PRINT 1917
207 GO TO 998
208 PRINT 1918
209 GO TO 998
210 PRINT 1919
211 C
212 PRINT 998,NRCRVS,NRPLTS
213 IF(NRCRVS .EQ. 0) GO TO 999
214 CALL PLOT(0.,0.,999)
215 STOP
216 C
217 1000 FORMAT('1')
218 1001 FORMAT(' ')
219 1002 FORMAT(20A4)
220 1003 FORMAT(1X,20A4)
221 1004 FORMAT('ADDITIONAL PLOT IDENTIFICATION: ',AB,1X,AB)
222 1020 FORMAT(1X,F7.0,3(2X,F8.0),2(2X,E10.0),2(2X,ES.0))
223 1022 FORMAT('OSLAB ',12,' R',F7.3,' F',F8.4,' A',F8.3,' C',F8.3,' M',
224 $
225 F6.3,' S',1PE10.3,' E',OPF5.1,' T',F5.1)
226 1023 FORMAT(11,2F9.0,11,4E15.0)
227 1024 FORMAT(/11X,' M ID THETA')
228 1025 FORMAT(11X,12,3X,11,OP2F10.5,12,2(1X,1P2E16.8)/
229 $
230 16X,
231 11,OP2F10.5,12,2(1X,1P2E16.8)
232 16X,
233 11,OP2F10.5,12,2(1X,1P2E16.8)
234 16X,
235 11,OP2F10.5,12,2(1X,1P2E16.8)
236 16X,
237 11,OP2F10.5,12,2(1X,1P2E16.8)

```

```

228          16X,      11,0P2F10.5,I',2(1X,1P2E16.8)
229  FORMAT('+',.80X,' MODES',13)
230  FORMAT('0***** ERROR IN CONTROL CARD')
231  FORMAT('0***** THIS DATA DECK IS MISSING THE FOUR FLAG IN 20')
232  FORMAT('0***** XVALS OUT OF ORDER')
233  FORMAT('0***** NRCURV MUST BE LESS THAN OR EQUAL TO 4')
234  FORMAT('0***** NUMBER OF SLABS LESS THAN 2')
235  FORMAT('0***** END OF DATA SET ON UNIT 5')
236  FORMAT('0***** ERROR IN DATA SEQUENCE')
237  FORMAT('0***** ITEM FLAG INCONSISTENT')
238  FORMAT('0***** SIZEY MUST BE LESS THAN OR EQUAL TO 9')
239  FORMAT('0***** NRPTS MUST BE LESS THAN OR EQUAL TO 501')
240  FORMAT('END OF JOB, ',12,' CURVES PLOTTED IN ',12,' GRAPHS')
241  END

```

```

1      SUBROUTINE MCSTEP
2
3      SUBROUTINE TO CALCULATE MODE CONVERSION COEFFICIENTS
4
5      IMPLICIT REAL*8 (A-H,O-Z)
6      COMMON/MC INPT/XTRA(3,20),TERM(20),FREQ,OMEGA,WAVENTO,MIK,
7      ALPHA,AK,AK13,KA23,KA23,NGSQ,NTHSQ,SKIP(3)
8      COMMON/MC STOR/A(20,20),FOFR(20),S(20),SKIP1(43),NRMODE,NRSLAB
9      COMMON/MC PLOT/ISKIP(69),NPRINT
10     COMMON NORM(20,20),CAPI(20),ANS(20),PS(20),
11     EXO(20),EYO(20),HXO(20),
12     PEXO(20),PEYO(20),PHXO(20),
13     EXT(20),EYT(20),HXT(20),HYT(20),TAU(20),
14     PEXT(20),PEYT(20),PHXT(20),PHYT(20),PTAU(20)
15     COMPLEX*16 THETAP,FOFR,XTRA,TERM,ANS,A,S,SSQ,SJ,SM,TJ,TM,PS,
16     QO,H10,H20,H1PRMO,H2PRMO,QT,H1T,H2T,H1PRMT,H2PRMT,
17     A1,A2,A3,A4,MIK,EY0J,EYOM,
18     FPRP,DFPRP,FPRL,DFPRL,MULT,ARGT,ARGO,ARGG,NORM,CAP1,
19     EXO,EXT,EYO,EYT,HXO,HXT,HYO,NGSQ,TAU,
20     PEXO,PEXT,PEYO,PEYT,PHXO,PHXT,PHYT,PNGSQ,PTAU,
21     ONE/(1.00,0.00)/.ZERO/(0.00,0.00)/,
22     W/(0.00,-1.4574954400)/
23     REAL*8 KA13,KA23,NTHSQ
24     INTEGER PNMODE
25
26     DO 90 M=1,NRMODE
27     THETAP=M
28     SSQ=S(M)**2
29     TM=CDSQRT(NGSQ-SSQ)
30     TAU(M)=TM
31     A2=DCPLX(0.00,KA13)*TM
32     A1=A2/NGSQ
33     QO=KA23*(ONE-SSQ)
34     CALL MDHMKL(QO,H10,H20,H1PRMO,H2PRMO,THETAP,'MCO')
35     EXO(M)=-TM/NGSQ
36     EYO(M)=FOFR(M)
37     HXO(M)=TM*FOFR(M)
38     HYO=ONE
39     QT=KA23*(NTHSQ-SSQ)
40     CALL MDHMKL(QT,H1T,H2T,H1PRMT,H2PRMT,THETAP,'MCT')
41     A3=H1T *H20 -H10 *H2T
42     A4=H1T *H2PRMO-H1PRMO*H2T
43     FPRP=A4-A1*A3
44     DFPRP=A4-A2*A3
45     A3=H1PRMT*H20 -H10 *H2PRMT
46     A4=H1PRMT*H2PRMO-H1PRMO*H2PRMT
47     DFPRP=A4-A1*A3
48     DFPRP=A4-A2*A3
49     EXT(M)=DCPLX(0.00,AK13)*DFPRP/W
50     EYT(M)=EYO(M)*FPRP/W
51     HXT(M)=DCPLX(0.00,-AK13)*EYO(M)*DFPRP/W
52     HYT(M)=FPRL/W
53     CONTINUE
54
55     IF(NRSLAB.EQ.1) GO TO 30
56
90
C

```

```

57 C INTEGRAL IN CURRENT SLAB
58 IF(NPRINT.GT. 2) PRINT 906,NRSLAB
59 DO 140 M=1,NRMODE
60 SM=S(M)
61 TM=TAU(M)
62 EYOM=EYO(M)
63 IF(NPRINT.GT. 2) PRINT 902
64 DO 140 J=1,NRMODE
65 IF(J.EQ. M) GO TO 120
66 SJ=S(J)
67 TJ=TAU(J)
68 EYOJ=EYO(J)
69 MULT=ONE/(MIK*(SU-SM))
70 ARGV=TERM(M)*(EY(M)*HXT(J)-EY(J)*HXT(M))
71 $ - (HYT(M)*EXT(J)-HYT(J)*EXT(M))
72 $ ARGQ=TLHM(M)*(EYO(M)*HXO(J)-EYO(J)*HXO(M))
73 $ - (EXO(J)-EXO(M))
74 ARGG=(ONE+EYOJ*EYOM)*(SU+SM)/(MIK*(TJ+TM))
75 GO TO 130
76 C MODES ARE EQUAL
77 120 MULT=SM*(2.DO/ALPHA)
78 SSO=SM**2
79 QO=ONE-SSO
80 QI=NTHSQ-SSQ
81 ARGV=TERM(M)*(QT*EY(M)*'2-HXT(M)**2)*(QT*HYT(M)**2-EXT(M)**2)
82 ARGQ=TERM(M)*(QO*EYO(M)*'2-HXO(M)**2)*(QO-EXO(M)**2)
83 ARGG=(ONE+EYOM**2)*SM/(MIK*TM)
84 NORM(J,M)=MULT*(ARGV-ARGQ)-ARGG
85 IF(NPRINT.GT. 2) PRINT 908,M,J,NORM(J,M)
86 140 CONTINUE
87 C
88 IF(NTH:Q.EQ. PNTHSQ) GO TO 300
89 C PREVIOUS SLAB HAD DIFFERENT TOPHT, MUST RECOMPUTE FIELDS
90 DO 200 J=1,PNMODE
91 THETAP=J
92 SSO=PS(J)**2
93 A2=DCPLX(0.DO,KA13)*PTAU(J)
94 A1=A2/PNGSQ
95 QO=KA23*(ONE-SSQ)
96 CALL MDHMKL(QO,H1O,H2O,H1PRMO,H2PRMO,THETAP,'MCPO')
97 QT=KA23*(NTHSQ-SSQ)
98 CALL MDHMKL(QT,H1T,H2T,H1PRMT,H2PRMT,THETAP,'MCPT')
99 A3=H1T *H2O -H1O *H2T
100 A4=H1T *H2P*HMO-H1PRMO*H2T
101 FPRL=A4-A1*A3
102 FPRP=A4-A2*A3
103 A3=H1PRMT*H2O -H1O *H2PRMT
104 A4=H1PRMT*H2P*HMO-H1PRMO*H2PRMT
105 DFPRL=A4-A1*A3
106 DFPRP=A4-A2*A3
107 PEY(J)=DCPLX(0.DO,AK13)*DFPRL/W
108 PEY(J)=PEYO(J)*FPRP/W
109 PHXT(J)=DCPLX(0.DO,-AK13)*PEYO(J)*DFPRP/W
110 PHXT(J)=FPRL/W
111 CONTINUE
112 200 C
113 C INTEGRALS ACROSS SLAB BOUNDARY

```

```

114 INIT=0
115 IF(NPRINT .GT. 1) PRINT 900,NRSLAB
116 DO 500 J=1,PNMODE
117 SU=PS(J)
118 SJR=SJ
119 SJI=SJ*(O.DO,-1.DO)
120 TJ=PTAU(J)
121 EY0J=PEY0(J)
122 IF(NPRINT .GT. 1) PRINT 902
123 DO 400 M=1,NRMODE
124 SM=S(M)
125 SMR=SM
126 SMI=SM*(O.DO,-1.DO)
127 TM=TAU(M)
128 EY0M=EY0(M)
129 IF(SMR .EQ. SUR .AND. SMI .EQ. SJI) GO TO 350
130 MULT=ONE/(MIK*(SJ-SM))
131 ARG1=TERM(M)*(EY0(M)*PHX1(J)-PEY0(J)*HXT(M))
132 ARG2=TERM(M)*(EY0(M)*PEXT(J)-PHXT(J)*EXT(M))
133 ARG3=TERM(M)*(EY0(M)*PHX0(J)-PEY0(J)*HX0(M))
134 ARG4=TERM(M)*(EY0(J)-PEX0(J)-EX0(M))
135 ARG5=(ONE+EY0J+EY0M)*(SU+SM)/(MIK*(TJ+TM))
136 GO TO 390
137 C MODES ARE EQUAL
138 MULT=SM*(2.DO/ALPHA)
139 SSQ=SM**2
140 QQ=ONE-SSQ
141 QT=NTHSQ-SSQ
142 ARG1=TERM(M)*(QT+EY0(M)**2-HXT(M)**2)+(QT*HXT(M)**2-EXT(M)**2)
143 ARG2=TERM(M)*(QQ+EY0(M)**2-HX0(M)**2)+(QQ-EX0(M)**2)
144 ARG3=(ONE+EY0M**2)*SM/(MIK*TM)
145 CAPI(M)=MULT*(ARG1-ARG2)-ARG3
146 IF(NPRINT .GT. 2) PRINT 910,M,J,CAPI(M)
147 CONTINUE
148 C
149 C CALCULATE CONVERSION COEFFICIENTS FOR HY
150 CALL CLINEQ(NORM,CAPI,ANS,NRMODE,20,INIT,ERR)
151 INIT=1
152 IF(NPRINT .GT. 2) PRINT 902
153 DO 430 M=1,NRMODE
154 A(J,M)=ANS(M)
155 IF(NPRINT .LT. 2) GO TO 430
156 AR=ANS(M)
157 AI=ANS(M)*(O.DO,-1.DO)
158 DB=10.*DLOG10(AR*AR+AI*AI)
159 ANG=ATAN2(AI,AR)*57.295779500
160 PRINT 903,M,J,AR,AI,DB,ANG
161 CONTINUE
162 CONTINUE
163 GO TO 50
164 C
165 C FIRST SLAB
166 DO 32 M=1,NRMODE
167 DO 32 J=1,NRMODE
168 IF(J .EQ. M) GO TO 31
169 A(J,M)=ZERO
170 GO TO 32
300 INIT=0
301 IF(NPRINT .GT. 1) PRINT 900,NRSLAB
302 DO 500 J=1,PNMODE
303 SU=PS(J)
304 SJR=SJ
305 SJI=SJ*(O.DO,-1.DO)
306 TJ=PTAU(J)
307 EY0J=PEY0(J)
308 IF(NPRINT .GT. 1) PRINT 902
309 DO 400 M=1,NRMODE
310 SM=S(M)
311 SMR=SM
312 SMI=SM*(O.DO,-1.DO)
313 TM=TAU(M)
314 EY0M=EY0(M)
315 IF(SMR .EQ. SUR .AND. SMI .EQ. SJI) GO TO 350
316 MULT=ONE/(MIK*(SJ-SM))
317 ARG1=TERM(M)*(EY0(M)*PHX1(J)-PEY0(J)*HXT(M))
318 ARG2=TERM(M)*(EY0(M)*PEXT(J)-PHXT(J)*EXT(M))
319 ARG3=TERM(M)*(EY0(M)*PHX0(J)-PEY0(J)*HX0(M))
320 ARG4=TERM(M)*(EY0(J)-PEX0(J)-EX0(M))
321 ARG5=(ONE+EY0J+EY0M)*(SU+SM)/(MIK*(TJ+TM))
322 GO TO 390
323 C MODES ARE EQUAL
324 MULT=SM*(2.DO/ALPHA)
325 SSQ=SM**2
326 QQ=ONE-SSQ
327 QT=NTHSQ-SSQ
328 ARG1=TERM(M)*(QT+EY0(M)**2-HXT(M)**2)+(QT*HXT(M)**2-EXT(M)**2)
329 ARG2=TERM(M)*(QQ+EY0(M)**2-HX0(M)**2)+(QQ-EX0(M)**2)
330 ARG3=(ONE+EY0M**2)*SM/(MIK*TM)
331 CAPI(M)=MULT*(ARG1-ARG2)-ARG3
332 IF(NPRINT .GT. 2) PRINT 910,M,J,CAPI(M)
333 CONTINUE
334 C
335 C CALCULATE CONVERSION COEFFICIENTS FOR HY
336 CALL CLINEQ(NORM,CAPI,ANS,NRMODE,20,INIT,ERR)
337 INIT=1
338 IF(NPRINT .GT. 2) PRINT 902
339 DO 430 M=1,NRMODE
340 A(J,M)=ANS(M)
341 IF(NPRINT .LT. 2) GO TO 430
342 AR=ANS(M)
343 AI=ANS(M)*(O.DO,-1.DO)
344 DB=10.*DLOG10(AR*AR+AI*AI)
345 ANG=ATAN2(AI,AR)*57.295779500
346 PRINT 903,M,J,AR,AI,DB,ANG
347 CONTINUE
348 CONTINUE
349 GO TO 50
350 C
351 C FIRST SLAB
352 DO 32 M=1,NRMODE
353 DO 32 J=1,NRMODE
354 IF(J .EQ. M) GO TO 31
355 A(J,M)=ZERO
356 GO TO 32
430 CONTINUE
500 CONTINUE
501 GO TO 50

```



```

57 C GET EXCITATION FACTORS AT END OF SLAB
58 SOLN B(J)=SOLN B(J)*CDEXP(MIKX*(S(J)-ONE))
59 TERM (J)=SOLN B(J)
60 M=M+1
61 X=XVAL
62
63 C GET DATA FOR NEXT SLAB
64 READ(4) STORE
65 MIKX=MIKX*XVAL
66 CALL HIGAIN(1,FREQ,SIGMA,EPSSR,ALPHA,NRMODE,TP,DBLE(RALT),HGR)
67
68 C IF(M.EQ.1) GO TO 685
69
70 C DO 681 J=1,NRMODE
71 C HY EXCITATION FACTOR
72 TA=(0.00,0.00)
73 DO 665 K=1,PNRMODE
74 TA=TA+TERM(K)*A(K,J)
75 SOLN B(J)=TA
76 IF(RCOMP.EQ.2) GO TO 671
77 C EZ EXCITATION FACTOR
78 TA=-S(J)*TA
79 GO TO 680
80 C EY EXCITATION FACTOR
81 IA=FOFR(J)*TA
82 SOLN A(J)=TA+HGR(RCOMP,J)
83 CONTINUE
84 GO TO 690
85
86 C FIRST SLAB
87 CALL HIGAIN(1,FREQ,SIGMA,EPSSR,ALPHA,NRMODE,TP,DBLE(TALT),HGT)
88 DO 689 J=1,NRMODE
89 C HY EXCITATION FACTOR
90 TA=(0.00,0.00)
91 DO 686 TCOMP=1,3
92 TA=TA+XTRA(TCOMP,J)*HGT(TCOMP,J)*T(TCOMP)
93 SOLN B(J)=TA
94 IF(RCOMP.EQ.2) GO TO 687
95 C EZ EXCITATION FACTOR
96 TA=-S(J)*TA
97 GO TO 688
98 C EY EXCITATION FACTOR
99 IA=FOFR(J)*TA
100 SOLN A(J)=TA+HGR(RCOMP,J)
101 CONTINUE
102 C DIST=X/1000.00
103 IF(INPRINT.EQ.0) GO TO 720
104
105 C PRINT MORE CONSTANTS TABLE
106 PRINT 1031,M,DIST
107 DO 692 J=1,NRMODE
108 SR=S(J)
109 SI=S(J)*MI
110 ATTEN=ACONST*SI
111 VOVERC=1.00/SR
112 WR=SOLN A(J)
113

```

```

114 W1=SOLN A(J),MI
115 WMI=ECUNST+10.00*DLOG10(WR**2+W1**2)
116 WAI=DATAN2(WI,WR)-1.570796326794900
117 PRINT 1032,J,ATTEN,VOVERC,WMI,WAI
118 CONTINUE
119
120 C
121 C GET SUM OF MODES
122 IF(RHD .GT. XVAL) GO TO 600
123 TA=0.00
124 MIKX=MIK*(RHO-X)
125 DO 730 K=1,NRMODE
126 TB=SOLN A(K)*CDEXP(MIKX*(S(K)-ONE))
127 TA=TA+TB
128 TA=TA*CONST/DSQRT((DABS(DSIN(RHD/6.36603))))
129
130 TDBI=TA*MI
131 PHS2=DATAN2(TDBI,TDBR)*57.295779500
132 IF(DABS(PHS1-PHS2) .LT. 180.00) GO TO 750
133 IF(PHS1 .GT. PHS2) GO TO 740
134 CYCLE=CYLE-360.00
135 GO TO 750
136 CYCLE=CYLE+360.00
137 PHS1=PHS2
138 ISUB=ISUB+1
139 R(ISUB)=RHO/1000.00
140 DR(ISUB)=10.*DLOG10(TDBR**2+TDBI**2)
141 ANG(ISUB)=PHS2+CYCLE
142 SUMOUT(ISUB)=TA
143 RHO=RHO+DEL RHO
144 IF(ISUB .LT. NRPTS) GO TO 720
145 RETURN
146
147 C
148 FOMMAT('1',20A4/1X,A1,' COMPONENT INCL =',F4.0,
149 ' THETA =',F5.0,' TALT =',F5.1,' RALT =',F5.1/
150 ' OSLAB RHO MODE ATTN V/C REL EXC 1')
151 FOMMAT(1X,13,F9.3)
152 FOMMAT(13X,13,F8.3,F9.5,2(F10.3,F7.3))
153 END

```



```

57 FK=FK+PHSMAX
58 OUT1(1)=OUT1(1)+PHSMAX
59 GO TO 36
60 IF(PHSMAX .EQ. 0.) GO TO 35
61 FK=FK-PHSMAX
62 OUT1(1)=OUT1(1)-PHSMAX
63 GO TO 36
64 FK=FK+PHSMIN
65 OUT1(1)=OUT1(1)+PHSMIN
66 UP(1)=.TRUE.
67 GO TO 31
68 CONTINUE
69 NPLOT=2
70 YMAX=PHSMAX
71 YMIN=PHSMIN
72 YINC=PHSINC
73
74
75 NRCRVS=NRCRVS+1
76 IF(KK .GT. 1) GO TO 109
77 IF(IR .GT. 0) GO TO 101
78 CALL SYMBOL(-1,0.,.1,DATIME,90.,16)
79 CALL PLOT(1.5,1.7,-3)
80 GO TO 102
81 CALL PLOT(OFFSET,0.,-3)
82 NRPLTS=NRPLTS+1
83 XP=0.
84 YP=-.4
85 CALL SYMBOL(XP,YP,.1,4HFMC ,0.,4)
86 XP=XP+0.5
87 CALL NUMBER(XP,YP,.1,FLOAT(NRPLTS),0.,-1)
88 XP=0.
89 YP=YP-.15
90 CALL SYM00L(XP,YP,.1,LABEL,0.,1)
91 XP=XP+0.2
92 CALL SYMBOL(XP,YP,.1,9HCOMPONENT,0.,9)
93 XP=XP+1.0
94 IF(NPLOT .EQ. 2) GO TO 103
95 CALL SYMBOL(XP,YP,.1,9HAMPLITUDE,0.,9)
96 XP=XP+1.1
97 CALL SYMBOL(XP,YP,.1,7HPOWER ,0.,7)
98 XP=XP+0.8
99 CALL NUMBER(XP,YP,.1, POWER ,0.,0)
100 XP=XP+0.6
101 GO TO 104
102 CALL SYMBOL(XP,YP,.1,14HRELATIVE PHASE,0.,14)
103 XP=XP+1.5
104 CALL SYMBOL(XP,YP,.1,6HFREQ = ,0.,6)
105 XP=XP+0.7
106 CALL NUMBER(XP,YP,.1,FREQ,0.,3)
107 XP=0.
108 YP=YP-.15
109 CALL SYMBOL(XP,YP,.1,6HINCL =,0.,6)
110 XP=XP+0.7
111 CALL NUMBER(XP,YP,.1, INCL ,0.,0)
112 XP=XP+0.6
113 CALL SYMBOL(XP,YP,.1,7HTheta =,0.,7)
114 XP=XP+0.8

```

```

114 CALL NUMBER(XP,YP,.1, THETA ,0.,0)
115 XP=XP+0.8
116 CALL SYMBOL(XP,YP,.1,6HTALT = ,0.,6)
117 XP=XP+0.7
118 CALL NUMBER(XP,YP,.1,TALT,0.,1)
119 XP=XP+0.7
120 CALL SYMBOL(XP,YP,.1,6HRALT = ,0.,6)
121 XP=XP+0.7
122 CALL NUMBER(XP,YP,.1,RALT,0.,1)
123 IF(BUMPID(1) .EQ. BLANK) GO TO 108
124 XP=0.
125 YP=YP-.15
126 CALL SYMBOL(XP,YP,.1,BUMPID(1),0.,4)
127 XP=XP+0.5
128 CALL SYMBOL(XP,YP,.1,BUMPID(2),0.,72)
129 CALL BURDER(SIZE,X,DMIN,DMAX,XINC,1,SIZEY,YMIN,YMAX,YINC,1)
130 GO TO 110
131 IF(IR .EQ. 0) GO TO 110
132 CALL PLOT(OFFSET,0.,-3)
133 C
134
135 XP=0.
136 YP=-.85-.15*KK
137 XL(1)=-1.1
138 XL(2)=-0.1
139 YL(1)=YP
140 YL(2)=YP
141 UL(1)=.FALSE.
142 UL(2)=.FALSE.
143 CALL CURVE(XL,YL,UL,2,0.,0.,1.,1.,KK)
144 CALL SYMBOL(XP,YP,.1,1D,0.,80)
145 SCALEX=(DMAX-DMIN)/SIZEY
146 SCALEY=(YMAX-YMIN)/SIZEY
147 CALL CURVE(D,OUT1,UP,NRPTS,DMIN,YMIN,SCALEX,SCALEY,KK)
148 IF(NPLOT .EQ. 1) GO TO 30
149 C
150 IF(IR .LT. 0) GO TO 999
151 IF(KK .EQ. NRCURV) GO TO 121
152 IF(IR .EQ. 0) GO TO 999
153 CALL PLOT(-OFFSET,0.,-3)
154 GO TO 999
155 CALL PLOT(0.,0.,-4)
156 LINE=0
157 RETURN
158 C
159 1000 FORMAT('1',20A4/1X,A1,' COMPONENT INCL =',F4.0, RALT =',F5.1/
160 $ , THETA =',F5.0,' TALT =',F5.1,'
161 $ 4(' DIST AMPLITUDE PHASE',7X))
162 1011 FORMAT(4(F7.3,2F10.4,5X))
END

```

```

1  SUBROUTINE BORDER(XLNG,XMIN,XMAX,XINC,NX,YLNG,YMIN,YMAX,YINC,NY)
2  DIMENSION XINC(NX),YINC(NY)
3  LOGICAL FY,FX
4  FX=.FALSE.
5  FY=.FALSE.
6  IF(NX.EQ.1) FX=.TRUE.
7  IF(NY.EQ.1) FY=.TRUE.
8  XT=XLNG-.1
9  YT=YLNG-.1
10 XSCALE=XLNG/(XMAX-XMIN)
11 YSCALE=YLNG/(YMAX-YMIN)
12 YM=ABS(YMIN)
13 YLN=-.4
14 IF(YM.GE.10.) YLN=YLN-.1
15 IF(YM.GE.100.) YLN=YLN-.1
16 IF(YM.GE.1000.) YLN=YLN-.1
17 IF(YMIN.LT.0.) YLN=YLN-.1
18 YM=ABS(YMAX)
19 YLM=-.4
20 IF(YM.GE.10.) YLM=YLM-.1
21 IF(YM.GE.100.) YLM=YLM-.1
22 IF(YM.GE.1000.) YLM=YLM-.1
23 IF(YMAX.LT.0.) YLM=YLM-.1
24 XM=ABS(XMAX)
25 XLM=-.3
26 IF(XM.GE.10.) XLM=XLM-.1
27 IF(XM.GE.100.) XLM=XLM-.1
28 IF(XM.GE.1000.) XLM=XLM-.1
29 IF(XMAX.LT.0.) XLM=XLM-.1
30 IF(FX) DX=XINC(1)
31 IF(FY) DY=YINC(1)
32 IY=1
33 YL=0.
34 CALL NUMBER(YLN,0.,.1,YMIN,0.,1)
35 CALL PLOT(0.,0.,3)
36 IF(FY) GO TO 110
37 YP=(YINC(IY)-YMIN)*YSCALE
38 GO TO 111
39 YL=YL+DY
40 YP=YL*YSCALE
41 IF(YP.LT.0.) GO TO 99
42 IF(YP.GE.YLNG) GO TO 11
43 CALL PLOT(0.,YP,2)
44 CALL PLOT(.1,YP,2)
45 CALL PLOT(0.,YP,2)
46 IF(FY) GO TO 110
47 IY=IY+1
48 IF(IY.LE.NY) GO TO 10
49 CALL PLOT(0.,YLNG,2)
50 CALL NUMBER(YLM,YLNG-.1,.1,YMAX,0.,1)
51 IX=1
52 XL=0.
53 IF(FX) GO TO 112
54 XP=(XINC(IX)-XMIN)*XSCALE
55 GO TO 120
56

```

```

57 XL=XL+DX
58 XP=XL*XSCALE
59 IF(XP .LT. 0.) GO TO 99
60 IF(XP .GE. XLNG) GO TO 13
61 CALL PLOT(XP,YLNG,2)
62 CALL PLOT(XP,YT,2)
63 CALL PLOT(XP,YLNG,2)
64 IF(FX) GO TO 112
65 IX=IX+1
66 IF(IX .LE. NX) GO TO 12
67 CALL PLOT(XLNG,YLNG,2)
68 IF(FY) GO TO 130
69 IY=IY-1
70 IF(IY .LE. 0) GO TO 15
71 YP=(YINC(IY)-YMIN)*YSCALE
72 GO TO 14
73 YL=YL-DY
74 YP=YL*YSCALE
75 IF(YP .LE. 0.) GO TO 15
76 CALL PLOT(XLNG,YP,2)
77 CALL PLOT(XT,YP,2)
78 CALL PLOT(XLNG,YP,2)
79 IF(FY) GO TO 130
80 GO TO 113
81 CALL PLOT(XLNG,0.,2)
82 CALL NUMBER(XLNG*XLNG,-.2,.1,XMAX,0.,1)
83 CALL PLOT(XLNG,0.,3)
84 IF(FX) GO TO 150
85 IX=IX-1
86 IF(IX .LE. 0) GO TO 17
87 XP=(XINC(IX)-XMIN)*XSCALE
88 GO TO 16
89 XL=XL-DX
90 XP=XL*XSCALE
91 IF(XP .LE. 0.) GO TO 17
92 CALL PLOT(XP,0.,2)
93 CALL PLOT(XP,.1,2)
94 CALL PLOT(XP,0.,2)
95 IF(FX) GO TO 150
96 GO TO 115
97 CALL PLOT(0.,0.,2)
98 CALL NUMBER(0.,-.2,.1,XMIN,0.,1)
99 RETURN
100 PRINT 100,XLNG,XMIN,XMAX,XINC(1),NX,YLNG,YMIN,YMAX,YINC(1),NY
101 FORMAT('0000 ERROR IN BORDER: XLNG, XMIN, XMAX, XINC(1), NX =',
102 1P4E15.5,15/24X,'YLANG, YMIN, YMAX, YINC(1), NY =',1P4E15.5,
103 15/'0000')
104 CALL PLOT(0.,0.,999)
105 STOP
106 END

```



```

57 DELY=DELY+DELR/RHO
58 DX 6=DELX*.1
59 DY 6=DELY*.1
60 IF(DR .EQ. 0.) GO TO 20
61 DX=DELX*DR/DELR
62 DY=DELY*DR/DELR
63 PX1=PX1+DX
64 PY1=PY1+DY
65 GO TO 21
66 IF(RHO2 .GT. RHO1) GO TO 38
67 PX1=PX1+DELX
68 PY1=PY1+DELY
69 CALL PLOT(PX1,PY1,IP)
70 IF(IKK .EQ. 6) CALL PLOT(PX1+DXG,PY1+DYG,2)
71 J=J+1
72 IP=IPEN(JD+MOD(J,JC))
73 RHO2=RHO2+DELR
74 GO TO 20
75 DR=0.
76 RHO1=0.
77 RHO2=DELR
78 GO TO 39
79 C PEN HAS BEEN UP. PREPARE TO LOWER PEN
80 CALL PLOT(PX2,PY2,3)
81 GO TO 39
82 CALL PLOT(PX2,PY2,IP)
83 DR=RHO2-RHO1
84 PX1=PX2
85 PY1=PY2
86 UP1=UP2
87 CONTINUE
88 RETURN
89 END

```

```

1  SUBROUTINE CLIN EQ (A, B, X, N, N DIM, IFLAG, ERR)
2
3  CLIN EQ USES L-U DECOMPOSITION TO
4  FIND THE TRIANGULAR MATRICES L, U
5  SUCH THAT  $L \cdot U = A$ . L AND U ARE
6  STORED IN A. THIS FORM IS USED WITH
7  BACK-SUBSTITUTION TO FIND THE SOLN
8  X OF  $A \cdot X = L \cdot U \cdot X = B$ .
9  N IS THE NUMBER OF EQUATIONS AND
10 N DIM IS THE DIMENSION OF ALL ARRAYS
11 IN THE PARAMETER LIST.
12
13 IF IFLAG = 0, L, U, AND X ARE
14 COMPUTED.
15 IF IFLAG IS NON-ZERO, IT IS ASSUMED
16 THAT L AND U HAVE BEEN COMPUTED IN
17 A PREVIOUS CALL AND ARE STILL STORED
18 IN A. THUS ONLY X IS COMPUTED.
19 ERR IS THE ESTIMATED RELATIVE
20 ERROR OF THE SOLUTION VECTOR.
21
22 COMPLEX*16 A, B, X, T
23 REAL*8 ERR
24 DIMENSION A(N DIM, N DIM), B(N DIM), X(N DIM)
25 DIMENSION IROW(51), Q(51)
26 DATA EPS /1.0E-15/
27
28 IF (N.GT.51) GO TO 900
29 IF (N.EQ.1) GO TO 850
30 IF (IFLAG.NE.0) GO TO 600
31 DO 050 I = 1, N
32   Q(I) = 0.0
33 DO 040 J = 1, N
34   QQ = CDABS (A(I,J))
35 040 IF (Q(I).LT.QQ) Q(I) = QQ
36 IF (Q(I).EQ.0.0) GO TO 901
37 050 CONTINUE
38 ERR = EPS
39 PPIV = 0.0
40 DO 100 I = 1, N
41   IROW(I) = I
42
43 DO 500 L = 1, N
44   PIVOT = 0.0
45   K = L - 1
46 DO 240 I = L, N
47   IF (K.LT.1) GO TO 230
48 DO 220 J = 1, K
49   A(I,L) = A(I,L) - A(J,L) * A(I,J)
50 F = CDABS (A(I,L)) / Q(I)
51 IF (PIVOT.GT.F) GO TO 240
52   PIVOT = F
53 NPIVOT = I
54 240 CONTINUE
55 IF (PIVOT.EQ.0.0) GO TO 901
56 IF (PPIV.LE.PIVOT) GO TO 250

```

```

57 ERR = ERR + PPIV / PIVOT
58 IF (ERR.GE.1.000) GO TO 901
59 PPIV = PIVOT
60 IF (NPIVOT.EQ.L) GO TO 280
61 Q(NPIVOT) = Q(L)
62 J = IROW(L)
63 IROW(L) = IROW(NPIVOT)
64 IROW(NPIVOT) = J
65 DO 260 I = 1,N
66 T = A(L,I)
67 A(L,I) = A(NPIVOT,I)
68 A(NPIVOT,I) = T
69 CONTINUE
70 260 IF (L.EQ.N) GO TO 500
71 T = (1.000,0.000) / A(L,L)
72 K = L + 1
73 M = L - 1
74 DO 450 I = K,N
75 IF (M.LT.1) GO TO 400
76 DO 350 J = 1,M
77 350 A(L,I) = A(L,I) - A(L,J) * A(J,I)
78 400 A(L,I) = T * A(L,I)
79 450 CONTINUE
80 CONTINUE
81 500 IF (ERR.GT.1.0D-5) PRINT 998, ERR
82
83
84
85
86
87
88
89
90
91
92
93
94
95
96
97
98
99
100
101
102
103
104
105
106
107
108
109
110
111
112
113

```

114
115
116
117

\$: CLIN EQ HAS DECOMPOSED AN ILL-CONDITIONED MATRIX. ,/.
\$: RESULTS WILL HAVE RELATIVE ERROR = , (E11.2)
999 FORMAT I'DERROR IN CLIN EQ, MATRIX SIZE GREATER THAN 51'
END

```

1 SUBROUTINE HTGAIN(IOPT,FREQ,SIGMA,EPSR,ALPHA,NRMODE,TP,Z,HG)
2 IMPLICIT REAL*8 (A-H,O-Z)
3 COMPLEX*16 TP(1),HG(3,1),HGO/(0.00,1.45749544D0)/,
4 S,C,SSO,CSQ,NGSQ,SQROOT,RATIO,A1,A2,A3,A4,
5 PO,H10,H20,H1PRMO,H2PRMO,PZ,H1Z,H2Z,H1PRMZ,H2PRMZ,EXPZ,
6 REAL*8 K,KA13,KA23
7 DATA DTR/1.745329252D-02/
8
9 C
10 OMEGA=6.2831853072D03*FREQ
11 NGSQ=DCMPLX(EPSR,-SIGMA/(8.85434D-12*OMEGA))
12 K=2.0958426D-02*FREQ
13 IF(ALPHA.EQ.0.00) GO TO 5
14 AK=ALPHA/K
15 AK13=DCXP(DLOG(AK)/3.00)
16 AK23=AK13**2
17 KA13=1.00/AK13
18 KA23=KA13**2
19 PI=KA23*ALPHA*Z
20 EXPZ=DCXP(.5D0*ALPHA*Z)
21 DO 20 M=1,NRMODE
22 S=DCSIN(TP(M)*DTR)
23 SSO=S*S
24 CSQ=ONE-SSO
25 SQROOT=CSQSQRT(NGSQ-SSQ)
26 TEST=TP(M)*I
27 IF(TEST.GT.10.00 .OR. ALPHA.EQ.0.00) GO TO 10
28 PO=KA23*CSQ
29 CALL MDHNKL(PO,H10,H20,H1PRMO,H2PRMO,TP(M),HG(1))
30 PZ=PO+PI
31 CALL MDHNKL(PZ,H1Z,H2Z,H1PRMZ,H2PRMZ,TP(M),HG(2))
32 A1=H10 *H2Z -H1Z *H20
33 A2=H1PRMO*H2Z -H1Z *H2PRMO
34 A3=H10 *H2PRMZ-H1PRMZ*H20
35 A4=H1PRMO*H2PRMZ-H1PRMZ*H2PRMO
36 RATIO=SQROOT/NGSQ
37 C=.5D0*AK23+KA13*MI*RATIO
38 HG(1,M)=EXPZ*(C*A1+A2)
39 HG(2,M)=KA13*MI*SQROOT*A1+A2
40 HG(3,M)=.5D0*AK*MI*HG(1,M)+AK13*MI*EXPZ*(C*A3+A4)
41 IF(IOPT.EQ.1) GO TO 20
42 HG(1,M)=HG(1,M)/HGO
43 HG(2,M)=HG(2,M)/HGO
44 HG(3,M)=HG(3,M)/((RATIO*HGO)
45 GO TO 20
46 C=CSQSQRT(CSQ)
47 EXPZ=CDEXP(DCMPLX(0.00,K*Z)*C)
48 A1=(NGSQ*C-SQROOT)/(NGSQ*C+SQROOT)
49 A2=(C-SQROOT)/(C+SQROOT)
50 HG(1,M)=EXPZ+A1/EXPZ
51 HG(2,M)=EXPZ+A2/EXPZ
52 HG(3,M)=(EXPZ-A1/EXPZ)*C
53 IF(IOPT.EQ.1) GO TO 20
54 HG(1,M)=HG(1,M)/(ONE+A1)
55 HG(2,M)=HG(2,M)/(ONE+A2)
56 HG(3,M)=HG(3,M)/((ONE-A1)*C)

```

CONTINUE
RETURN
END

20

57
58
59

SUBROUTINE MOHNKL (Z,M1,M2,M1PRIME,M2PRIME,THETA,IDBG)

1
2
3
4
5
6
7
8
9
10
11
12
13
14
15
16
17
18
19
20
21
22
23
24
25
26
27
28
29
30
31
32
33
34
35
36
37
38
39
40
41
42
43
44
45
46
47
48
49
50
51
52
53
54
55
56

DATA A / 9.30436716929229440190-01, 3.10145572309743149110+01,
 2.0676371487316208970+02, 5.74343652425450274490+02,
 8.70217655190076172340+02, 8.28778719228643973200+02,
 5.41685437404342465420+02, 2.57945446303020221110+02,
 9.34504950663116742310+01, 2.6626351870740666620+01,
 6.12100043005610727940+00, 1.15928038448032334720+00,
 1.84012759441321160160-01, 2.48330309637410480030-02,
 2.80420800972602103000-03, 2.91334142396567861380-04,
 2.58274948933127536460-05, 2.02560587398531400630-06,
 1.41557363660748707340-07, 8.86950900130004431240-09,
 5.01102203463279330090-10, 2.56580749341156855260-11,
 1.19618064960912206660-12, 5.09080924812072031850-14,
 1.99483929895177163880-15, 7.18861008631269057970-17,
 2.39380955255167851120-18, 7.38030108812246452550-20,
 2.1194208514075287620-21, 5.6653858632471340830-23/
 6.7829072514275804560-01, 1.13049787524045980330+01,
 5.3032321543076097040+01, 1.53371031778654158410+02,
 7.47422182157184006310+01, 1.27809193148878465030+02,
 1.07853128730410390060+01, 3.2359386215231170600+01,
 6.1360373630972235950-01, 2.05325737403202090050+00,
 1.6422939954065644650-02, 1.09376780098212519650-01,
 2.33167787640721305710-04, 2.10550512239571339110-03,
 1.91567080450163745950-06, 1.44469094758796188390-07,
 9.72861244166977697300-09, 5.88542797439187958910-10,
 3.21608086032343146440-11, 1.59527820452551163510-12,
 7.21518662291050037780-14, 2.987657444763967170-15,
 1.2946984700953559130-19, 3.9809598637666916030-18,
 1.09202239049148706360-22, 3.89851993405460882280-21,
 4.65218358461614724100-01, 6.20291144619406298220+00,
 2.58454643591452623020+01, 5.22130593114045703920+01,
 6.21584039421432900120+01, 4.07516893663908218970+01,
 2.70842718702171232280+01, 1.12150194079574009090+01,
 3.59455750255044900220+00, 9.18150064508416091470-01,
 1.91281263438253351990-01, 3.31222966994378097400-02,
 4.84244103792950434440-03, 6.05683682042464583210-04,
 6.5550182039277680830-05, 6.190591177439506086120-06,
 5.16549097866255071190-07, 3.02204081084021509860-08,
 2.52781006537051262770-09, 1.50330661038983801410-10,
 8.08229360424044091570-12, 3.9473961437110544710-13,
 1.75908919060105126750-14, 7.18142147622637789200-16,
 2.69572878236725896410-17, 9.3385725495154618650-19,
 2.99226194060959813150-20, 8.9015675760516207010-22,
 2.4644285051250333750-23, 6.36560209353610574090-25/
 6.7829872514275884560-01, 4.52199150096183921310+01,
 3.76832625060153267760+02, 1.19629404787350243440+03,
 1.99382341312250405460+03, 2.04494709038205543750+03,
 1.42010214609864960900+03, 7.11830649673508574630+02,

DATA B / 9.30436716929229440190-01, 3.10145572309743149110+01,
 2.0676371487316208970+02, 5.74343652425450274490+02,
 8.70217655190076172340+02, 8.28778719228643973200+02,
 5.41685437404342465420+02, 2.57945446303020221110+02,
 9.34504950663116742310+01, 2.6626351870740666620+01,
 6.12100043005610727940+00, 1.15928038448032334720+00,
 1.84012759441321160160-01, 2.48330309637410480030-02,
 2.80420800972602103000-03, 2.91334142396567861380-04,
 2.58274948933127536460-05, 2.02560587398531400630-06,
 1.41557363660748707340-07, 8.86950900130004431240-09,
 5.01102203463279330090-10, 2.56580749341156855260-11,
 1.19618064960912206660-12, 5.09080924812072031850-14,
 1.99483929895177163880-15, 7.18861008631269057970-17,
 2.39380955255167851120-18, 7.38030108812246452550-20,
 2.1194208514075287620-21, 5.6653858632471340830-23/
 6.7829072514275804560-01, 1.13049787524045980330+01,
 5.3032321543076097040+01, 1.53371031778654158410+02,
 7.47422182157184006310+01, 1.27809193148878465030+02,
 1.07853128730410390060+01, 3.2359386215231170600+01,
 6.1360373630972235950-01, 2.05325737403202090050+00,
 1.6422939954065644650-02, 1.09376780098212519650-01,
 2.33167787640721305710-04, 2.10550512239571339110-03,
 1.91567080450163745950-06, 1.44469094758796188390-07,
 9.72861244166977697300-09, 5.88542797439187958910-10,
 3.21608086032343146440-11, 1.59527820452551163510-12,
 7.21518662291050037780-14, 2.987657444763967170-15,
 1.2946984700953559130-19, 3.9809598637666916030-18,
 1.09202239049148706360-22, 3.89851993405460882280-21,
 4.65218358461614724100-01, 6.20291144619406298220+00,
 2.58454643591452623020+01, 5.22130593114045703920+01,
 6.21584039421432900120+01, 4.07516893663908218970+01,
 2.70842718702171232280+01, 1.12150194079574009090+01,
 3.59455750255044900220+00, 9.18150064508416091470-01,
 1.91281263438253351990-01, 3.31222966994378097400-02,
 4.84244103792950434440-03, 6.05683682042464583210-04,
 6.5550182039277680830-05, 6.190591177439506086120-06,
 5.16549097866255071190-07, 3.02204081084021509860-08,
 2.52781006537051262770-09, 1.50330661038983801410-10,
 8.08229360424044091570-12, 3.9473961437110544710-13,
 1.75908919060105126750-14, 7.18142147622637789200-16,
 2.69572878236725896410-17, 9.3385725495154618650-19,
 2.99226194060959813150-20, 8.9015675760516207010-22,
 2.4644285051250333750-23, 6.36560209353610574090-25/
 6.7829872514275884560-01, 4.52199150096183921310+01,
 3.76832625060153267760+02, 1.19629404787350243440+03,
 1.99382341312250405460+03, 2.04494709038205543750+03,
 1.42010214609864960900+03, 7.11830649673508574630+02,

DATA C / 9.30436716929229440190-01, 3.10145572309743149110+01,
 2.0676371487316208970+02, 5.74343652425450274490+02,
 8.70217655190076172340+02, 8.28778719228643973200+02,
 5.41685437404342465420+02, 2.57945446303020221110+02,
 9.34504950663116742310+01, 2.6626351870740666620+01,
 6.12100043005610727940+00, 1.15928038448032334720+00,
 1.84012759441321160160-01, 2.48330309637410480030-02,
 2.80420800972602103000-03, 2.91334142396567861380-04,
 2.58274948933127536460-05, 2.02560587398531400630-06,
 1.41557363660748707340-07, 8.86950900130004431240-09,
 5.01102203463279330090-10, 2.56580749341156855260-11,
 1.19618064960912206660-12, 5.09080924812072031850-14,
 1.99483929895177163880-15, 7.18861008631269057970-17,
 2.39380955255167851120-18, 7.38030108812246452550-20,
 2.1194208514075287620-21, 5.6653858632471340830-23/
 6.7829072514275804560-01, 1.13049787524045980330+01,
 5.3032321543076097040+01, 1.53371031778654158410+02,
 7.47422182157184006310+01, 1.27809193148878465030+02,
 1.07853128730410390060+01, 3.2359386215231170600+01,
 6.1360373630972235950-01, 2.05325737403202090050+00,
 1.6422939954065644650-02, 1.09376780098212519650-01,
 2.33167787640721305710-04, 2.10550512239571339110-03,
 1.91567080450163745950-06, 1.44469094758796188390-07,
 9.72861244166977697300-09, 5.88542797439187958910-10,
 3.21608086032343146440-11, 1.59527820452551163510-12,
 7.21518662291050037780-14, 2.987657444763967170-15,
 1.2946984700953559130-19, 3.9809598637666916030-18,
 1.09202239049148706360-22, 3.89851993405460882280-21,
 4.65218358461614724100-01, 6.20291144619406298220+00,
 2.58454643591452623020+01, 5.22130593114045703920+01,
 6.21584039421432900120+01, 4.07516893663908218970+01,
 2.70842718702171232280+01, 1.12150194079574009090+01,
 3.59455750255044900220+00, 9.18150064508416091470-01,
 1.91281263438253351990-01, 3.31222966994378097400-02,
 4.84244103792950434440-03, 6.05683682042464583210-04,
 6.5550182039277680830-05, 6.190591177439506086120-06,
 5.16549097866255071190-07, 3.02204081084021509860-08,
 2.52781006537051262770-09, 1.50330661038983801410-10,
 8.08229360424044091570-12, 3.9473961437110544710-13,
 1.75908919060105126750-14, 7.18142147622637789200-16,
 2.69572878236725896410-17, 9.3385725495154618650-19,
 2.99226194060959813150-20, 8.9015675760516207010-22,
 2.4644285051250333750-23, 6.36560209353610574090-25/
 6.7829872514275884560-01, 4.52199150096183921310+01,
 3.76832625060153267760+02, 1.19629404787350243440+03,
 1.99382341312250405460+03, 2.04494709038205543750+03,
 1.42010214609864960900+03, 7.11830649673508574630+02,

DATA D / 9.30436716929229440190-01, 3.10145572309743149110+01,
 2.0676371487316208970+02, 5.74343652425450274490+02,
 8.70217655190076172340+02, 8.28778719228643973200+02,
 5.41685437404342465420+02, 2.57945446303020221110+02,
 9.34504950663116742310+01, 2.6626351870740666620+01,
 6.12100043005610727940+00, 1.15928038448032334720+00,
 1.84012759441321160160-01, 2.48330309637410480030-02,
 2.80420800972602103000-03, 2.91334142396567861380-04,
 2.58274948933127536460-05, 2.02560587398531400630-06,
 1.41557363660748707340-07, 8.86950900130004431240-09,
 5.01102203463279330090-10, 2.56580749341156855260-11,
 1.19618064960912206660-12, 5.09080924812072031850-14,
 1.99483929895177163880-15, 7.18861008631269057970-17,
 2.39380955255167851120-18, 7.38030108812246452550-20,
 2.1194208514075287620-21, 5.6653858632471340830-23/
 6.7829072514275804560-01, 1.13049787524045980330+01,
 5.3032321543076097040+01, 1.53371031778654158410+02,
 7.47422182157184006310+01, 1.27809193148878465030+02,
 1.07853128730410390060+01, 3.2359386215231170600+01,
 6.1360373630972235950-01, 2.05325737403202090050+00,
 1.6422939954065644650-02, 1.09376780098212519650-01,
 2.33167787640721305710-04, 2.10550512239571339110-03,
 1.91567080450163745950-06, 1.44469094758796188390-07,
 9.72861244166977697300-09, 5.88542797439187958910-10,
 3.21608086032343146440-11, 1.59527820452551163510-12,
 7.21518662291050037780-14, 2.987657444763967170-15,
 1.2946984700953559130-19, 3.9809598637666916030-18,
 1.09202239049148706360-22, 3.89851993405460882280-21,
 4.65218358461614724100-01, 6.20291144619406298220+00,
 2.58454643591452623020+01, 5.22130593114045703920+01,
 6.21584039421432900120+01, 4.07516893663908218970+01,
 2.70842718702171232280+01, 1.12150194079574009090+01,
 3.59455750255044900220+00, 9.18150064508416091470-01,
 1.91281263438253351990-01, 3.31222966994378097400-02,
 4.84244103792950434440-03, 6.05683682042464583210-04,
 6.5550182039277680830-05, 6.190591177439506086120-06,
 5.16549097866255071190-07, 3.02204081084021509860-08,
 2.52781006537051262770-09, 1.50330661038983801410-10,
 8.08229360424044091570-12, 3.9473961437110544710-13,
 1.75908919060105126750-14, 7.18142147622637789200-16,
 2.69572878236725896410-17, 9.3385725495154618650-19,
 2.99226194060959813150-20, 8.9015675760516207010-22,
 2.4644285051250333750-23, 6.36560209353610574090-25/
 6.7829872514275884560-01, 4.52199150096183921310+01,
 3.76832625060153267760+02, 1.19629404787350243440+03,
 1.99382341312250405460+03, 2.04494709038205543750+03,
 1.42010214609864960900+03, 7.11830649673508574630+02,

```

57 2.6963282184602597 1920+02, 7.9891206472890585111D+01,
58 1.9021715826801392940+01, 3.71881052333922566820+00,
59 6.07648778323402885720-01, 8.4220204895828535644D-02,
60 1.0026214868551016149D-02, 1.0363012784032058021D-03,
61 9.3867869420580235442D-05, 7.5124345274574017960D-06,
62 5.3507368429103773360D-07, 3.413542251472901631D-08,
63 1.9610093247972931935D-09, 1.020970508063274472D-10,
64 4.834176377350352579D-12, 2.0913590211334783723D-13,
65 8.2990437346566602039D-15, 3.031614149646268564D-16,
66 1.0228117913786331176D-17, 3.196780345924792364D-19,
67 9.2821903191776400453D-21, 2.5103962999804300309D-22,
68 1.0416666666666666663D-01, 8.35503472222222222116D-02,
69 1.2822657455632716019D-01, 2.9104902646414046315D-01,
70 8.8162726744375764074D-01, 3.3214012818627675264D+00,
71 1.4995762986862554546D+01, 7.092301301158517530D+01,
72 4.7445153886U26431887D+02, 3.207490090906619001D+03,
73 2.4006549640U74004605D+04, 1.989231191695097912D+05,
74 1.791902007753438063D+06, 1.7484377180034121023D+07,
75 1.8370737967633072970D+08, 2.0679040329451551508D+09,
76 2.482751937593588472D+10, 3.1669454901734887315D+11,
77 4.2771126865134715582D+12, 6.0971132411392560749D+13,
78 9.1486942234356396792D+14, 1.441352517009350101D+16,
79 2.3780844395175757942D+17, 4.104601600946921885D+18,
80 7.3900049415704853993D+19, 1.3859220004603943141D+21,
81 2.7030825930275761623D+22, 5.4747478619645573335D+23,
82 1.1498937014386333524D+25, 2.5014180692753603969D+26/

```

C

```

DATA 1/(0.00,1.00)//,MI/(0.00,-1.00)/
DATA ONE/(1.00,0.00)//,TWO/(2.00,0.00)//,ZERO/(0.00,0.00)//
DATA ROOT3/(1.732050807568880,0.00)//
DATA ALPHA/(8.53667218838951D-1,0.00)//
DATA CONST1/( 2.58819045102522D-01,-9.65925826289067D-01)//
DATA CONST2/( 2.58819045102522D-01, 9.65925826289067D-01)//
DATA CONST3/(-9.65925826289067D-01, 2.58819045102522D-01)//
DATA CONST4/(-9.65925826289067D-01,-2.58819045102522D-01)//

```

C

```

ZPOWER=ONE
SUM3=ZLRO
SUM4=ZLRO
ZMAG=CDABS(Z)
IF(ZMAG.GT. 6.1D0) GO TO 70
SUM1=ZLRO
SUM2=ZERO
ZTERM=-Z**3/(200.00,0.00)
DO 50 M=1,30
SUM1=SUM1+DCPLX(A(M),0.00)*ZPOWER
SUM2=SUM2+DCPLX(B(M),0.00)*ZPOWER
SUM3=SUM3+DCPLX(C(M),0.00)*ZPOWER
SUM4=SUM4+DCPLX(D(M),0.00)*ZPOWER
SUM4=SUM4+TERM4
IF(DABS(PART1(1))/PART2(1)) .LE. 1.0D-17 .AND.
DABS(PART1(2))/PART2(2)) .LE. 1.0D-17) GO TO 60
ZPOWER=ZPOWER*ZTERM
CONTINUE
GM2F=1*(Z*SUM2-TWO*SUM1)/ROOT3
GPMFP=1*(SUM4-TWO*Z*SUM3)/ROOT3
M1=Z*SUM2+GM2F

```

50

60

```

114 H2=H1-TWO*GM2F
115 H1PRME=SUM4*GPMFP
116 H2PRME=H1PRME-TWO*GPMFP
117 GO TO 999
118
119 C
120 70
121 MPOWER=ONE
122 SUM1=ONE
123 SUM2=ONE
124 RTZ=CDSORT(Z)
125 SORTZ=RTZ*Z
126 ZTERM=1/SORTZB
127 MTERM=-ZTERM
128 DM=ZERO
129 TERM3=ONE
130 DO 80 M=1,30
131 ZPOWER=ZPOWER*ZTERM
132 MPOWER=MPOWER*MTERM
133 DM=DM*ONE
134 TERM1=DCMLX(CAP(M),0.00)*ZPOWER
135 TERM2=DCMLX(CAP(M),0.00)*MPOWER
136 IF(CDAUS(TERM2/TERM3) .GE. 1.00) GO TO 81
137 SUM1=SUM1+TERM1
138 SUM2=SUM2+TERM2
139 SUM3=SUM3+DM*TERM1
140 TERM4=DM*TERM2
141 SUM4=SUM4+TERM4
142 IF(DABS(PART1(1)/PART2(1)) .LE. 1.D-17 .AND.
143 $ DABS(PART1(2)/PART2(2)) .LE. 1.D-17) GO TO 81
144 TERM3=TERM2
145 CONTINUE
146 ZTERM=(1-1.500,0.00)/Z
147 SUM3=SUM3*ZTERM
148 SUM4=SUM4*ZTERM
149 TERM1=((-0.2500,0.00)-1*SQRTZB1)/Z
150 TERM2=((-0.2500,0.00)+1*SQRTZB1)/Z
151 EXP1=CDEXP((0.00,0.6666666666666667D0)*SQRTZB)
152 EXP2=CONST1*EXP1
153 EXP3=CONST2/EXP1
154 EXP4=CONST3*EXP1
155 EXP5=CONST4/EXP1
156 ZTERM=ALPHA/COSORT(RTZ)
157 TERM4=Z
158 IF(PART1(1) .GE. 0.00 .OR. PART1(2) .GE. 0.00) GO TO 90
159 H1=ZTERM*(EXP2*SUM2+EXP5*SUM1)
160 H1PRME=ZTERM*(EXP2*(SUM2*TERM2+SUM4)+EXP5*(SUM1+TERM1+SUM3))
161 GO TO 110
162 H1=ZTERM*EXP2*SUM2
163 H1PRME=ZTERM*EXP2*(SUM2*TERM2+SUM4)
164 IF(PART1(1) .GE. 0.00 .OR. PART1(2) .LT. 0.00) GO TO 120
165 H2=ZTERM*(EXP3*SUM1+EXP4*SUM2)
166 H2PRME=ZTERM*(EXP3*(SUM1+TERM1+SUM3)+EXP4*(SUM2+TERM2+SUM4))
167 GO TO 999
168 H2=ZTERM*EXP3*SUM1
169 H2PRME=ZTERM*EXP3*(SUM1+TERM1+SUM3)
170 C
171 C
172 CALCULATE WRONSKIAN AS PARTIAL CHECK ON VALIDITY
173 SUM4=H1*H2PRME-H1PRME*H2

```

```
171 IF(DABS(PART2(1))) .LE. 1.D-8 .AND.  
172 $ QABS(PART2(2))+1.4574954104046100) .LE. 1.D-8) GO TO 1000  
173 PRINT 1001,SUM4,THETA,DBG  
174 RETURN  
175 $  
176 $ ***** POSSIBLE ERROR IN MOHMKL: W = ,1P2E15.6,  
177 $ FOR THETA = ,0P2F10.4, AT ,A4)  
END
```

APPENDIX B:

BUMP

```

1  PROGRAM 'BUMP'
2
3  PROGRAM TO READ SEVERAL RADIALS WITH. SAY, VARYING M'.
4  THIS PROGRAM THEN GENERATES A SERIES OF DATA SETS COMPATIBLE
5  WITH FASTMC INPUT. THESE DATA SETS CAN BE USED TO GENERATE
6  A SERIES OF MODE SUMS TO SHOW THE EFFECT OF VARYING, SAY, THE
7  IONOSPHERE ALONG A PATH FOR WHICH THE GROUND CONDUCTIVITY OR
8  THE MAGNETIC FIELD VARIES SIGNIFICANTLY.
9
10 LOGICAL DEBUG/.FALSE./
11 CHARACTER*4 BCD,SAVE,ID
12 DIMENSION BCD(20), INDEX(7, 801), SAVE(81,20), HPRIME(7), ID(20)
13
14 C RH00 = START DISTANCE OF BUMP
15 C RHOL = END DISTANCE OF BUMP
16 C DRHO = INTERVAL BETWEEN BUMPS
17 C DRHO1 = DISTANCE INCREMENT BETWEEN HPRIME DATA SETS
18 C DRHO2 = LENGTH OF BOTTOM OF BUMP
19 C RHOMAX = TOTAL PATH LENGTH
20
21 C HPRIME = IONOSPHERIC HEIGHT PARAMETER FOR EACH DATA SET
22
23 C
24 C
25 C
26 C
27 C
28 C
29 C...SET UP RANDOM ACCESS FILES
30 DEFINE FILE 11 ( 801,1229,U,U1)
31 DEFINE FILE 12 ( 801,1229,U,U2)
32 DEFINE FILE 13 ( 801,1229,U,U3)
33 DEFINE FILE 14 ( 801,1229,U,U4)
34 DEFINE FILE 15 ( 801,1229,U,U5)
35 DEFINE FILE 16 ( 801,1229,U,U6)
36 DEFINE FILE 17 ( 801,1229,U,U7)
37
38 C...SET UP LOGICAL FILE FOR OUTPUT FILE
39 CALL FACSF('USE 2,OUTPUT . ')
40
41 C
42 MF=10
43 MR=0
44
45 READ(5,1000,END=900) BCD
46 PRINT 1001,BCD
47 IF(SUBSTR(BCD(1),1,4) .EQ. 'DATA') GO TO 100
48 IF(SUBSTR(BCD(1),1,4) .EQ. 'STAR') GO TO 200
49 IF(SUBSTR(BCD(1),1,4) .EQ. 'NAME') GO TO 20
50 IF(SUBSTR(BCD(1),1,4) .EQ. 'ID ') GO TO 30
51 GO TO 10
52
53 C...READ NAMED LIST DATA
54 READ DATUM
55 DRHO=SIGN(DRHO,RHOL-RH00)
56 PRINT DATUM
57 GO TO 9
58
59 C
60
61 C
62 C
63 C
64 C
65 C
66 C
67 C
68 C
69 C
70 C
71 C
72 C
73 C
74 C
75 C
76 C
77 C
78 C
79 C
80 C
81 C
82 C
83 C
84 C
85 C
86 C
87 C
88 C
89 C
90 C
91 C
92 C
93 C
94 C
95 C
96 C
97 C
98 C
99 C
100 C

```

DATA
START
NAMELIST
ID

```

57 C...ID FOR OUTPUT FILE
58 ID(1)='BLIMP'
59 READ 1000,(ID(1),1,2,19)
60 GO TO 10
61
62 C...READ INPUT DATA FOR MPRIME(MR)
63 DATA IS TO BE STORED IN RANDOM ACCESS FILE MF
64 MF=MF+1
65 MR=MR+1
66 IF(MR .GT. 7) GO TO 800
67 T=MPRIME(MR)
68 READ 1000,BCD
69 PRINT 1001,BCD
70 NR=0
71 I1=1
72 I2=0
73 READ 1100,R,F,A,C,B,S,E
74 IF(R .EQ. 40.) GO TO 110
75 IF(NR .EQ. 0) GO TO 103
76
77 C...CALCULATE RECORD NUMBER FOR RANDOM ACCESS FILE
78 C BASED ON 5 KM RESOLUTION
79 I2=R*20.+0.99
80 DO 102 I=I1,I2
81 INDEX(MR,I)=NR
82 NR=NR+1
83 F1=I2
84 PRINT 1100,R,F,A,C,B,S,E,F1
85 NM=0
86 NN=NM+1
87
88 C...DATA FOR EACH INPUT DISTANCE IS READ AND STORED AS LITERAL DATA
89 C A MAXIMUM OF 30 MODES MAY BE INPUT
90 IF(NM .GT. 61) GO TO 801
91 READ 1000,(SAVE(NM,I),I=1,20)
92 IF(SUBSTR(SAVE(NM,1),1,4) .EQ. ' ') GO TO 105
93 GO TO 104
94 WRITE(MF,NR) R,F,A,C,B,S,E,I,NM,SAVE
95 I1=I2+1
96 GO TO 101
97 DO 111 I=I1,IMAX
98 INDEX(MR,I)=NR
99 LASTM=NR
100 GO TO 10
101
102 C...BEGIN
103 RMO1=RMO0
104 CHECK FOR ID CARD
105 IF(SUBSTR(ID(1),1,4) .EQ. ' ') GO TO 201
106 WRITE(2,1000) ID
107 C...INITIALIZE FILE AND RECORD INDICES
108 MF=1
109 MR=1
110 INC=1
111 RLAST=0.
112 RMO=RMO1
113 IF(DEBUG) PRINT 1002, RMO,DRMO1,DRMO2,(MPRIME(1),I=1,LASTM)
114 WRITE(2,1200) RMO,DRMO1,DRMO2,(MPRIME(1),I=1,LASTM)

```

```

114
115
116
117
118
119
120
121
122
123
124
125
126
127
128
129
130
131
132
133
134
135
136
137
138
139
140
141
142
143
144
145
146
147
148
149
150
151
152
153
154
155
156
157
158
159
160
161
162
163
164
165
166
167
168
169
170

11=1
N1=INDEX(MR,1)
IF(RHO.GT. RHOMAX) RHO=RHO+RHO*20+.99
IF(I2.LT. 1) GO TO 220
IF(I2.GT. IMAX) I2=IMAX
N2=INDEX(MR,I2)
IF(DEBUG) PRINT 1003,MR,I1,I2,N1,N2
DO 210 N=N1,N2
READ(MF,N) R,F,A,C,B,S,E,T,NM,SAVE
IF(N.GT. N1) GO TO 207
R1=R
IF(R.GE. RLAST) GO TO 208
C...ADJUST R VALUES TO CORRESPOND TO BEGINNING OF CURRENT STEP
C USE DATA FROM PREVIOUS INPUT R VALUE
C EXAMPLE: SUPPOSE DATA WAS INPUT AT RHO=1.0 AND 1.2 MM.
C IF AN R VALUE GT 1.0 AND LT 1.2 MM IS REQUIRED, THEN THE
C PROGRAM WILL USE THE DATA FROM 1.0 MM AT THIS R VALUE.

DR=R-R1
R1=R
R=RLAST+DR
GO TO 209
R1=R
208 IF(DEBUG) PRINT 1100,R,F,A,C,B,S,E,T
209 WRITE(2,1000) R,F,A,C,B,S,E,T
210 WRITE(2,1000) ((SAVE(M,I),I=1,20),M=1,NM)
RLAST=RHO
IF(RHO.EQ. RHOMAX) GO TO 290
(I2.EQ. IMAX) GO TO 290
I1=I2+1
MF=MF+INC
MR=MR+INC
IF(MR.EQ. LASTM) GO TO 230
IF(MR.GT. LASTM) GO TO 240
IF(MR.EQ. 1) GO TO 250
IF(MR.LT. 1) GO TO 290
RHO=RHO+DRHO1
GO TO 202
C
230 RHO=RHO+DRHO2
GO TO 202
240 MF=MF-2
MR=MR-2
INC--1
GO TO 221
RHO=40.
GO TO 202
C
290 WRITE(2,1201)
RHO1=RHO1+DRHO
IF(DRHO.LT. 0.) GO TO 291
IF(RHO1.GT. RHO1) GO TO 9
GO TO 201
IF(RHO1.LT. RHO1) GO TO 9
GO TO 201

```

```

171 C
172 800 PRINT 1800
173 GO TO 900
174 801 PRINT 1801
175 STOP
176 FORMAT(20A4)
177 FORMAT(1X,20A4)
178 1001 FORMAT('DRHO1=',F5.2,' DRHO2=',F5.2,' H1=',F4.0)
179 1002 FORMAT('ORHO=',F5.2,' DRHO1=',F5.2,' DRHO2=',F5.2,' H1=',F4.0)
180 1003 FORMAT(80X,5I5)
181 1100 FORMAT(1X,F7.3,2X,F8.4,2(2X,F8.3),2(2X,1PE10.3),2(2X,0PF5.1))
182 1200 FORMAT('DATA',/,'RHO=',F5.2,' DRHO1=',F5.2,' DRHO2=',F5.2,' H1=',F4.0)
183 1201 FORMAT('R 40.1')
184 1800 FORMAT('0T00 MANY HPRIMES')
185 1801 FORMAT('0T00 MANY MODES')
186 END

```